ADSORPTION OF FLEXIBLE POLYELECTROLYTES

A theoretical and experimental study of polystyrene sulfonate adsorption on polyoxymethylene single crystals

Promotoren: dr. G.J. Fleer,
hoogleraar in de fysische- en kolloidchemie

dr. B.H. Bijsterbosch
hoogleraar in de fysische- en kolloidchemie

J. Papenhuijzen

ADSORPTION OF FLEXIBLE POLYELECTROLYTES

A theoretical and experimental study of polystyrene sulfonate adsorption on polyoxymethylene single crystals

Proefschrift
ter verkrijging van de graad van
doctor in de landbouwwetenschappen,
op gezag van de rector magnificus,
dr. C.C. Oosterlee,
in het openbaar te verdedigen
op vrijdag 15 maart 1985
des namiddags te vier uur in de aula
van de Landbouwhogeschool te Wageningen

ISN=221049-03

ELLINGEN.

Na "God" is "democratisch" waarschijnlijk het meest misbruikte woord.

Op een laag-energetisch, electrisch neutraal oppervlak adsorbeert een geladen polymeer wezenlijk anders dan op de meeste gangbare oppervlakken, die hoog-energetisch zijn en/of tegengesteld geladen aan het polyelectrolyt.

Dit proefschrift, hoofdstuk 4.

. Viscositeitsmetingen wijzen uit dat in de reeks polystyreen-sulfonaat ijkmonsters voor gelpermeatie chromatografie (Chemical Pressure Co.) het materiaal met het hoogste molecuulgewicht niet voldoet aan de specificitaties.

Dit proefschrift, hoofdstuk 3.

. In hun artikel over adsorptie van polyoxyethylnonylfenolen vinden Furlong en Aston onder bepaalde omstandigheden desorptie met toenemende concentratie adsorbaat. De oorzaak van dit artefact kan liggen in de spectrofotometrische concentratiebepaling, aangezien de extinctiecoëfficient van polyoxyethylnonylfenol verschuift bij overschrijding van de kritische micelvormingsconcentratie.

Furlong, D.N. en Aston, J.R.. Colloids and Surfaces 4, 121 (1982).
Dit proefschrift, hoofdstuk 2.

5. Zeise e.a. leggen ten onrechte een verband tussen de acute giftigheid en de carcinogeniteit van een verbinding.

Zeise, L., Wilson, R. en Crouch, E.. Risk Analysis 4, 187 (1984).

6. Voor de ozon afkomstig van een fotocopieermachine in een geventileerde ruimte beschrijft Nijman het evenwicht tussen vorming, afvoer en ontleding.
De auteur brengt echter de afbraakreactie foutief in rekening, en overschat aldus de werkelijk aanwezige ozonconcentratie in de buurt van het apparaat en daarmee de gezondheidsrisico's verbonden aan de bediening ervan.

Nijman, F., De Veiligheid 59 , 449 (1983).

7. In Nederland zijn naar verhouding veel onderzoeksafdelingen gevestigd van grote, multinationale ondernemingen. De afbouw van het wetenschappelijk onderwijs onder de vlag van de tweefasenstructuur geeft geen aanleiding tot al te groot optimisme over het voortbestaan van deze situatie.

8. Gezien de afnemende bevolkingsgroei vormen de jeugdige werklozen van nu een onmisbaar arbeidspotentieel voor de toekomst.

9. De voortvarende aanpak van de zogenoemde kleine criminaliteit, die de VVD voorstaat, steekt schril af bij de terughoudende reactie van deze partij op de RSV-affaire.

10. De aanschaf van een jonge rashond is alleen dan verantwoord als het betreffende ras tenminste tien jaar "uit" is.

11. Hoewel vaak een kleurrijk centrum voor watertoerisme, is elk grindgat in ecologisch opzicht een zwart gat in het landschap.

    Dekkers, M. en den Hengst, J. "Waterrijk", P 73,
    Het Spectrum B.V., Utrecht, 1981.

12. Aan de oplossing van de internationale schuldencrisis dienen de veroorzakers, schuldenlanden én geldschieters, naar draagkracht mee te werken.

J. Papenhuijzen
ADSORPTION OF FLEXIBLE POLYELECTROLYTES
A theoretical and experimental study of polystyrene sulfonate adsorption on polyoxymethylene single crystals.

Wageningen, 15 maart 1985.

Voor Annemiek

Voorwoord

Met dit proefschrift is een onderzoek afgesloten waarin velen binnen en buiten de vakgroep Fysische en Kolloïdchemie van de Landbouwhogeschool hebben bijgedragen.

Als promotor en begeleider speelde Gerard Fleer een sleutelrol. Altijd nam hij de tijd om de laatste ontwikkelingen te bespreken, en zijn adviezen zijn van wezenlijk belang geweest voor de planning van de verschillende fasen van het project. Tijdens het schrijven van het proefschrift was zijn kritisch commentaar op de opeenvolgende versies van het manuscript een grote steun. Bert Bijsterbosch gaf als tweede promotor mede richting aan de werkzaamheden. Van zijn brede ervaring en overzicht over het vakgebied had ik vooral in de afronding veel profijt.

Een goed begrip van de theorie van polyelectrolytadsorptie dank ik aan de vele gesprekken hierover met Henk van der Schee en Jan Scheutjens. Met genoegen denk ik ook terug aan de stimulerende discussies met Luuk Koopal.

Ten behoeve van de experimenten verzorgden Willem van Maanen en Ben Spee de aanwezigheid van alle chemicaliën en glaswerk. Martien Cohen Stuart maakte me bekend met een bestaande procedure voor het kristalliseren van polyoxymethyleen. Bij het karakteriseren van polyoxymethyleenkristallen verleende Joop Groenewegen van de vakgroep Virologie assistentie met de electronenmicroscopie. Ton Hustings (Dutch State Mines) en Joost Moonen (Universiteit van Utrecht) verrichtten respectievelijk dichtheids- en SAXS metingen aan de kristallen. Ab van der Linde heeft de oppervlaktelading van de kristallen gemeten, en Anton Korteweg het BET oppervlak. Thonie van den Boomgaard bracht me op het idee om een niet-ionogene surfactant te gebruiken ter bepaling van het specifiek oppervlak van kristallen van polyoxymethyleen in suspensie. Het leeuwendeel van de adsorptiemetingen heb ik kunnen overlaten aan Harco Klunder, die deze nauwkeurig en met toewijding uitvoerde. In dit proefschrift nemen zijn resultaten een voorname plaats in. Voorts dank ik Hugo Jongejan van de vakgroep Organische Chemie voor de elementen analyses aan polystyreensulfonaat, en Henny van Beek, Louis Verhagen en Gert Buurman bij wie ik altijd kon aankloppen om technische ondersteuning. Nauwgezet en zorgvuldig tekende en fotografeerde de laatstgenoemde bovendien de figuren.

TABLE OF CONTENTS

CHAPTER 1

Introduction

General

The behaviour of polymers at solid/liquid interfaces has been an important topic in the literature over the past decades. Recently, rapid progress in the theory of homopolymer adsorption has yielded a quantitative understanding of the adsorption behaviour for this simple type of polymer. When specific intra-molecular interactions are absent, a chain of a homopolymer may be considered to be completely flexible and, consequently, it behaves in solution as a random coil. When such a coil comes into contact with an adsorbing surface, many segments may attach to it. Due to the large number of contacts, significant adsorption occurs even if the free energy of adsorption per segment is small. Upon adsorption, the conformation of a flexible polymer molecule changes drastically. An adsorbed chain can be regarded as an alternating sequence of trains of segments in direct contact with the surface and loops in which non-adsorbed segments are surrounded by solvent. At either end of the molecule free dangling tails may be present. The affinity of the individual segments for the surface is the driving force in the adsorption process. It overcompensates the loss in translational and conformational entropy upon adsorption, as well as effects due to the effective excluded volume of the segments. The effective segmental excluded volume depends, for uncharged polymers, entirely on nearest neighbour interactions. The combination of these interactions with entropic factors, which is necessary to describe polymer adsorption theoretically, is now well established.

For polyelectrolytes the same factors play a role but, in addition, we have to account also for long range electrostatic interactions: segment-segment repulsion and the interaction between segmental and surface charges. The relative importance of these depends on the concentration of small ions. Due to screening effects, a high

concentration of indifferent electrolyte diminishes the magnitude of electrostatic interactions. The occurrence of nearest neighbour interactions along with long range electrostatic terms makes the theoretical description of the adsorption of polyelectrolytes essentially more difficult than for uncharged polymers.

Understanding the factors involved in polyelectrolyte adsorption and the way in which their effects are balanced may eventually be useful with respect to the practical application of polyelectrolytes in numerous fields. For example, the rate of crystallization of salts such as $CaSO_4$, $CaCO_3$ and $BaSO_4$ from a supersaturated solution is drastically reduced by the presence of adsorbed polyelectrolyte on the growing crystals. The final amount of precipitate is not affected, as the polyelectrolyte concentration is too low to influence its solubility. Retarded precipitation of these salts may be important in steam boilers and in flue gas desulphurification plants where $CaSO_4$ is produced by treating flue gas containing SO_x with lime water.

Polyelectrolytes may also be used to remove finely dispersed matter, e.g., from the effluent of water purification plants. Suspended particles are often too small to sediment as such. Sedimentation may in this case be enhanced by inducing flocculation. However, flocculation is often prevented by the presence of a surface charge, giving rise to repulsive forces between the particles. Flocculation can now be achieved by adding a polyelectrolyte flocculant in low concentrations. Adsorbing on more than one particle at the same time, the long polyelectrolyte molecules can form bridges, and as a result large flocs develop that settle readily. Also, the flocs can easily be separated by filtration, due to their stability and open structure. An alternative application of the same principle is in the improvement of soil structure. The formation of loose aggregates of soil particles upon adsorption of water-soluble polymers will enhance the water retention and the circulation of air, as well as the resistance to erosion.

Theories for polymer and polyelectrolyte adsorption

The first analysis of the adsorption behaviour of interacting chains was given independently by Hoeve (1) and Silberberg (2). The purpose of any polymer adsorption theory is to derive an expression for the free energy of adsorption. The quality of the theory depends on the assumptions that are made to arrive at such an expression. Hoeve treated the loops as random walks and Silberberg used a lattice model. Both theories neglect end effect (tails) and in both models an a priori (but different) assumption was used for the variation of the segment concentration as a function of the distance from the surface. Recently, Fleer and Lyklema (3) demonstrated that both approaches lead to very similar results, despite the differences in the underlying assumptions.

Using a similar lattice formalism as Silberberg, Roe (4) derived a more elaborate theory which was recently refined by Scheutjens and Fleer (5). For a given set of parameters the latter two models not only yield the adsorbed amount and layer thickness, but also the segmental concentration profile perpendicular to the surface, without any a priori assumption about its shape. The theory of Scheutjens and Fleer is the only approach, so far, in which the effects of tails are accounted for.

Polyelectrolyte adsorption can be described by adding an electrostatic term to the adsorption free energy function that holds for uncharged polymers. In such an analysis, it is assumed that the non-electrostatic and electrostatic contributions in the model are mutually independent. Hesselink (6) extended Hoeve's approach according to this principle. Van der Schee and Lyklema (7) derived a more sophisticated expression for the electrostatic adsorption free energy in a lattice model, that may be incorporated in the Roe theory and in that of Scheutjens and Fleer. In the application of Van der Schee's theory, we will only consider the first option, because the numerical complications involved with the latter have not yet been solved completely.

Objective and choice of the system

The aim of the present work is to compare experimental results on well-defined systems with the theory of Van der Schee and Lyklema for polyelectrolyte adsorption, based on the Roe model. For this purpose, adsorption measurements with strong polyelectrolytes are most suitable, as in this case the dissociation of the charged groups, and therefore the charge density along the chain, is not influenced by the local segment concentration. Consequently, variations in the dissociation of the polyelectrolyte segments as a function of the distance to the surface do not have to be taken into account. In addition, the adsorbate should be homodisperse. A low M_w/M_n ratio is important, as heterodispersity may give rise to complications, due to preferential adsorption of long chains over shorter ones (8). In order to facilitate interpretation of experimental results, it is desirable that the adsorbent is uncharged and has a homogeneous surface. A charged surface gives complications because a layer of adsorbed polyelectrolyte will influence the surface charge density. It affects the local activity of potential determining ions (Donnan effect) and/or their specific adsorption behaviour. An inhomogeneous surface has the disadvantage that the distribution of adsorption energies over the surface is usually unknown, so that the results cannot be interpreted unambiguously.

So far, experimental data obtained with strong polyelectrolytes are very scarce. Only in one case have the effects of variations in the chain length and in the concentrations of polyelectrolyte and indifferent electrolyte been studied systematically. This has been done by Marra et al. (9) who measured the adsorption of polystyrene sulfonate (PSS) on preheated silica. However, the surface of this adsorbent is heterogeneous and might also carry some surface charge.

In this work we present systematic polyelectrolyte adsorption data obtained by using a better defined surface which is virtually uncharged. Polyoxymethylene (POM) single crystals were selected as the adsorbent. Roe et al. (10) described a procedure to prepare these crystals, hexagonal platelets of uniform thickness, by careful recrystallization of POM from dilute solution in cyclohexanol. In this way, a chemically homogeneous surface is obtained which consists entirely of ether groups and is essentially uncharged.

As the adsorbate we used PSS, which is a strong, negatively charged polyelectrolyte that can be purchased as virtually homodisperse samples. Concentration determinations are greatly facilitated by the presence of a chromophore with a strong absorption band at 226 nm.

Outline of this study

In chapter 2 we describe the preparation of POM crystals. The method applied is based on that given by Roe et al., but we incorporated a number of improvements. Characterization of the crystals involved measurement of the thickness, density, specific surface area and surface charge density.

Ten PSS samples of different molecular weight were obtained ex Pressure Chemical Co. Chapter 3 deals with their characterization by means of elemental analysis, measurement of the extinction coefficient for two different absorption bands and viscometry. From the results it is concluded that only five samples are sufficiently reliable.

In chapter 4 we give adsorption data as a function of polyelectrolyte concentration, ionic strength and chain length. Most remarkable are the rounded isotherms found on POM, whereas on positively charged hematite high-affinity behaviour was established. We ascribe the difference to the fact that POM crystals present a low-energy, uncharged surface whereas the hematite surface is highly-energetic, carrying a charge of opposite sign to that of the polyelectrolyte. This interpretation is corroborated by adsorption data for PSS on POM crystals as a function of chain length and ionic strength, and by theoretical and experimental data taken from the literature.

The theories of Hesselink and Van der Schee and Lyklema are discussed in chapter 5. We carried out systematic calculations with the latter model and assessed the significance of the various parameters in determining theoretical trends.

Finally, chapter 6 is dedicated to the comparison between theory and experiment. Qualitatively, the model reproduces the measured dependence of the adsorbed amount on ionic strength and chain length. From this we conclude that the theory correctly combines electrostatic interactions and entropic terms. However, experimental isotherms are

rounded whereas theoretically high-affinity behaviour is found. The quantitative difference between theory and experiment is only of the order of 35 %, which is gratifying when we consider the large number of model parameters and the uncertainty in their estimates.

References

1. Hoeve, C.A.J., J. Polym. Sci. (C) 34, 1 (1971).
2. Silberberg, A., J. Chem. Phys. 48, 2835 (1968).
3. Fleer, G.J., and Lyklema, J., in "Adsorption from Solution at the Solid/Liquid Interface" (G.D. Parfitt and C.H. Rochester, Eds.), p. 153. Academic Press, London, 1983.
4. Roe, R.-J., J. Chem. Phys. 60, 4192 (1974).
5. Scheutjens, J.M.H.M., and Fleer, G.J., J. Phys. Chem. 83, 1619 (1979) and 84, 178 (1980).
6. Hesselink, F.Th., J. Colloid Interface Sci. 60, 448 (1977).
7. Van der Schee, H.A., and Lyklema, J., J. Phys. Chem., submitted.
8. Cohen Stuart, M.A., Scheutjens, J.M.H.M., and Fleer, G.J., J. Polym. Sci. Polym. Phys. Ed. 18, 559 (1980).
9. Marra, J., Van der Schee, H.A., Fleer, G.J., and Lyklema, J., in "Adsorption from Solution," (R.H. Ottewill, C.H. Rochester and A.L. Smith, Eds.), p. 245. Academic Press, London, 1983.
10. Roe, R.-J., Shastri, R., and Wille, W., J. Colloid Interface Sci. 84, 346 (1981).

CHAPTER 2

Preparation and Characterization of Polymer Single Crystals for Use as Adsorbent

---

Introduction

Under suitable conditions many linear homopolymers and some simple copolymers can be crystallized from dilute solution to form single crystals of lamellar morphology (1,2). In this way a solid of large surface area is obtained that may be suspended in various liquids, making the polymer-solution interface accessible for adsorption studies by means of the depletion technique. This was recognized by Roe et al. (3), who prepared single crystals of polyoxymethylene and measured adsorption of proteins from aqueous solution. For such experiments POM is suitable because of its relatively large density (> 1.25 g/cc (4)) and its insolubility in water. A distinct advantage of POM single crystals in adsorption studies is the homogeneous, uncharged surface.

When adsorption is to be measured by a depletion method, large amounts of crystals are needed. Sofar, the major part of the work done on polymer crystals was concerned with morphological studies (5,6,7). For this purpose minimal amounts of crystals are required, and only Roe et al. (3) explicitly describe a method for large scale preparation. In the present paper, we follow essentially their method, but a number of improvements are incorporated. In addition, we characterized the POM crystals by several techniques. We measured the specific surface area of the crystals by three methods: from the lamellar thickness as found with electron microscopy or small angle X-ray scattering, from nitrogen adsorption, and through adsorption of a surfactant from aqueous solution. In order to check whether any charged groups are present on the crystal surface, we carried out streaming potential measurements. The crystal density was determined using a helium pycnometer.

Properties of polymer single crystals

In the past two decades it has become apparent (8) that the solid state of flexible homopolymers (or regular copolymers) is often dominated by either one of two distinct states:

* The amorphous state, where no crystalline ordering can be detected, although a certain regularity has often been found (9).
* The crystalline state, which consists of ordered arrays of unit cells, characteristic for a given polymer. Each unit cell comprises several monomeric units and each polymer chain traverses many of these repeating units: crystalline ordering is independent of the chain length. Dimensions of unit cells are given by Geil (10) and Wunderlich (11).

The relative importance of either state depends on polymeric properties and on the mode of solidification (12). For instance, highly crystalline solids are formed from polymers consisting of simple monomeric units (without bulky side groups) that are allowed to crystallize slowly.

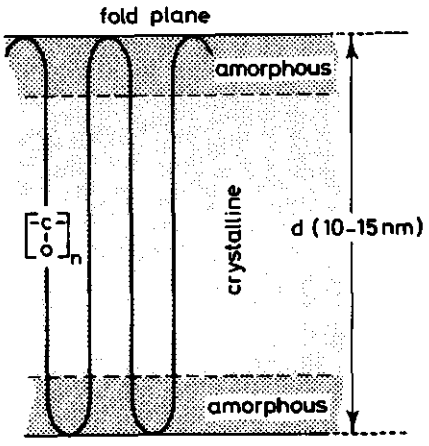

Figure 1: Schematic representation of the structure of a single crystal.

From dilute solutions of many polymers symmetric lamellar crystals can be grown. Each lamella may have lateral dimensions up to some square microns, whereas thicknesses are in the range between 5 and 50 nm. The polymer chains are oriented perpendicular to the large planes, which means that each chain is folded several times (see

fig. 1). This feature represents a major characteristic of such polymer crystals and has two important consequences:

* The middle region of a lamella consists of highly crystalline polymer that is sandwiched between two fold layers of amorphous nature. Thus the overall density of the crystal will be between the densities of purely amorphous and purely crystalline material (13).
* By its nature the fold-surface is not suitable as a growth face in a developing crystal (14). Crystal growth only occurs at the edges of the lamella and involves folding of randomly coiled chains from solution to fit into the lattice of the growth face presented.

When the crystallization temperature is not too low the formation of folded-chain crystals is a steady state process in which chain folding is the rate controlling factor (15). Under these conditions regularly shaped crystals are formed, e.g. lozenges in the case of polyethylene and hexagons in the case of POM (see fig. 2a). At lower temperatures the crystallization process will be diffusion controlled and more complicated branched (dendritic) structures are formed. Still lower crystallization temperatures cause solidification in an uncontrolled way. At too high polymer concentrations the formation of multilayer crystals becomes more important (6). Multilayer structures develop as growth spirals, starting from crystal imperfections (see fig. 3). In practice, therefore, the polymer concentration chosen represents a compromise between maximal yield and minimal occurrence of multilayer formation (3,6,7).

The thickness (fold length) is determined only by the type of polymer, the type of solvent and the crystallization temperature, and not by such factors as concentration or molecular weight of the crystallizing polymer (16). At temperatures below the dissolution temperature of the polymer in the solvent, the thickness increases with crystallization temperature. Once a crystal is formed, its shape and thickness are preserved upon cooling. The thickness can only be changed by heating the crystal above its temperature of formation, through annealing (5,17,18).

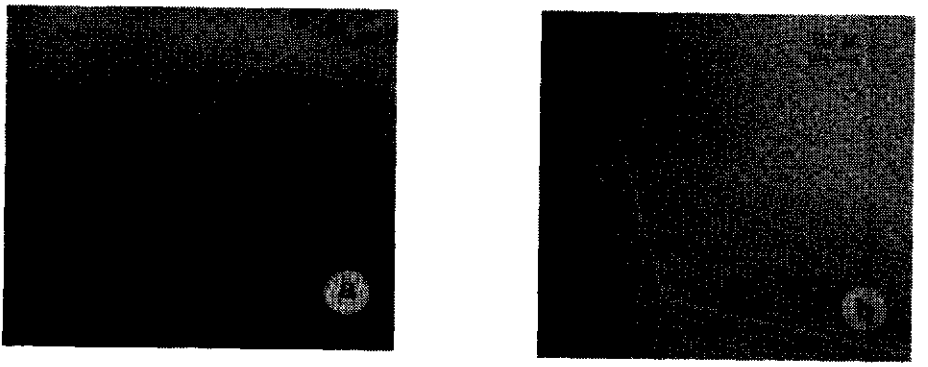

Figure 2: POM single crystals, shadowed unilaterally with Au/Pd. (a) grown at 135 °C. (b) grown at 141 °C. Note the thin, additional edge (between the arrows) that is formed when, after crystallization at 141 °C, low-molecular-weight material precipitates upon cooling of the suspension.

Figure 3: Spiral growth in a crystal grown at 135 °C. The only physical connection between the successive layers is at the center of the pyramid.

Preparation of POM single crystals

Polymer single crystals may be prepared by recrystallization from dilute solution, by means of the self-seeding technique. In this method, which was originally proposed by Blundell and Keller (6), most of the polymer is dissolved until a visually transparent solution is obtained. If the final temperature of the solution is chosen not too

high, the mixture still contains many submicroscopic crystalline nuclei (seeds). When the seeding suspension is quenched to the crystallization temperature each seed will become the nucleus of a lamellar crystal.

In the present work single crystals are prepared from polyoxymethylene (DELRIN 500 NC 10, ex Dupont). Each polymer chain carries an acetate endgroup to prevent degradation, so the general structure is: $(CH_2O)_n$-COCH , with n = 1500 for DELRIN 500 (19). Two crystallization procedures have been described in the literature: Khoury and Barnes (7) crystallized POM from o-dichlorobenzene and Roe et al. (3) used cyclohexanol as the solvent. Apart from the choice of the solvent, both procedures differ on minor other points. We employed the method of Roe et al. because these authors prepared large batches of crystals for use as adsorbent. Their method can be summarized as follows:

1) Finely dispersed POM is obtained by boiling 4 g. of POM-pellets with 400 ml. of cyclohexanol (1 % w/v) at about 160 °C. After dissolution of the polymer, the temperature is lowered to 140 °C and the polymer solidifies in an uncontrolled way, forming a kind of gel-like substance in which also solvent is included.
2) The seeding suspension is prepared by heating the system very slowly (10 °C/h or less (6)) until at 155 °C the suspension becomes optically transparent.
3) The seeding suspension is transferred rapidly to 9 volumes of cyclohexanol kept in a separate vessel at 143 °C, and isothermal crystallization is allowed to proceed at 144.5 °C.
4) When crystallization is complete, the suspension is allowed to cool to room temperature, and the crystals may be transferred to another solvent. This is achieved by a procedure of repeated solvent exchanges, in which the crystals are not allowed to become dry (once dried, they cannot be resuspended). Exchange of cyclohexanol with miscible organic solvents is straightforward. However, exchange for water, with which cyclohexanol is only partially miscible, requires an intermediate step: Roe et al. replaced cyclohexanol by acetone and, subsequently, acetone by water.

We found that this procedure can be improved in a number of ways:

* At all stages involving elevated temperatures (steps 1, 2 and 3), a nitrogen atmosphere should be maintained over the solution in order to

minimize oxydation of the solvent. We found that after longer periods of time oxydation of cyclohexanol by atmospheric oxygen becomes noticeable. This oxydation is probably the reason that Roe et al. used a rather short time of crystallization (1.5 h). Under nitrogen atmosphere, this could be extended to 24 h, according to general practice (7).

* Another difference involves homogenizing the solution throughout the crystallization process (step 3) by gentle stirring. In a nitrogen atmosphere there is no risk of enhanced oxidation of cyclohexanol, and at low stirrer speed anomalous crystallization does not occur. Indeed electron microscopic observations did never reveal the presence of any fibrillar structures, which have been reported to form at higher stirrer speed (20).

* A further modification concerns the crystallization temperature (step 3). Roe et al. crystallized POM at 144.5 °C, at which temperature only long polymer molecules will crystallize (21). As the POM-sample is heterodisperse, a considerable amount of polymer remains in solution and upon cooling the shorter chains crystallize at their respective crystallization temperatures. This gives rise to thin, irregular edges on the previously formed crystals, because the fold length decreases with decreasing crystallization temperature. Figure 2b illustrates this phenomenon. The occurrence of thin edges on the crystals may give rise to some additional surface heterogeneity, because the surface energy of a crystal is directly related to the fold length (22). One possibility to avoid these edges is to wash the crystals, after crystallization, with hot solvent. However, the washing procedure is rather complicated if a nitrogen atmosphere has to be maintained. Moreover, the washing process cannot be very efficient as the POM crystals form a voluminous sediment. For these reasons it was decided to omit the hot washing step and instead lower the crystallization temperature to 135 °C. Now virtually all low molecular weight polymer is incorporated in the crystals at the crystallization temperature. Fig. 2a shows that the thin edges referred to above are no longer noticeable. Also the morphology of the crystals is still hexagonal, and not dendritic, indicating that chain folding is still the rate controlling factor in the crystallization process. In fig. 4 the crystallization procedure

finally settled upon is graphically illustrated.

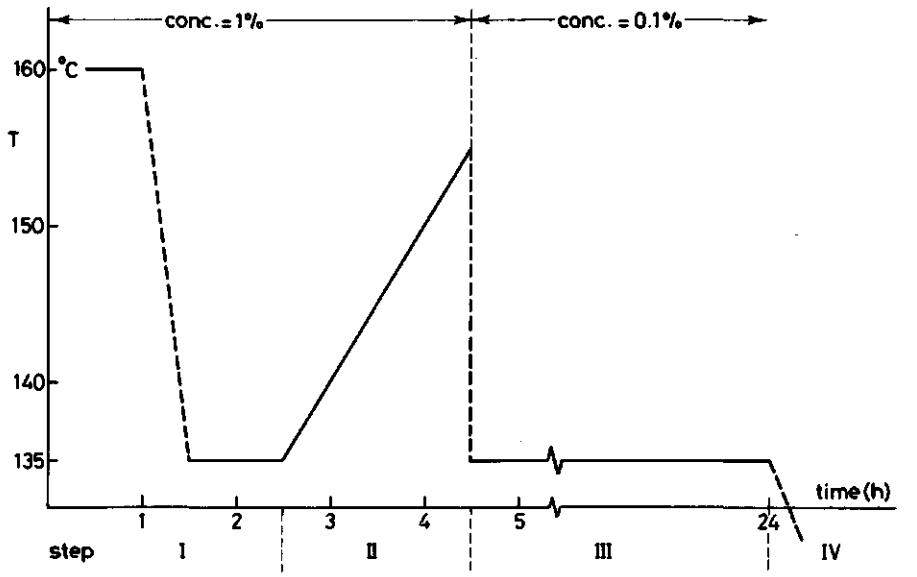

Figure 4: Manipulation of temperature and concentration in a typical recrystallization experiment.

Washing with hot solvent, apart from being cumbersome and inefficient, is also superfluous when purification of the newly formed crystals is concerned. In the original POM sample no impurities could be detected by elemental analysis: the carbon content was 40.17% (theoretically 40.00%) and the hydrogen content was 6.64% (theoretically 6.71%). Any traces of contamination that might nevertheless be present would be removed during the crystal preparation, which in fact involves both recrystallization (step 3) and extensive rinsing with organic solvent and water (step 4).

* As the intermediate solvent in the exchange of cyclohexanol for water (step 4), we employed ethanol instead of acetone. Ethanol was chosen because, unlike acetone, it is a non-solvent for POM (23). Acetone might cause some swelling of the crystals (19).
* Finally, when replacing ethanol by water special precautions have to be taken in order to prevent that by mixing of ethanol (or, for that matter, acetone) and water tiny air bubbles are formed. As ethanol is

gradually replaced by water these bubbles stick to the water/solid interface and cause the crystals to flotate. This always occurs when water is poured or syphoned into a crystal suspension, as soon as the water content of the medium is high enough, even when freshly boiled water is used. Flotation can only be avoided when heated water (40 °C) is syphoned very slowly (1 l/h) into a cooled suspension (8 °C). This method works well because the added water cools quickly so that, after mixing, the concentration of dissolved air is well below its saturation value at the lower temperature. Analogously, any occurring flotation can be eliminated by first heating the flotated suspension to 40 °C to drive out some excess air, and subsequent cooling to 8 °C.

The suspension of POM-crystals in water should be handled carefully in order to prevent flotation: stocks should not be agitated or poured from one vessel into another. However, they may be stirred carefully or transferred slowly by means of a syphon.

Characterization of POM single crystals

The regular shape of the crystals is determined by the hexagonal ordering of crystalline POM-chains in the core of the lammellae (see fig. 1). The dimensions of the crystals depend upon crystallization conditions, the lateral size usually being of the order of 1 µm and the thickness about 10 nm. From these numbers it is clear that the edges contribute only negligibly (around 1 %) to the entire surface area. Assuming that each lamella has two fold planes exposed to the surrounding medium, we can calculate the area per gram of POM from the crystal thickness d and density ρ only:

$$A_{sp} = \frac{2}{\rho d} \qquad [1]$$

The thickness can be determined by electron microscopy and by small angle X-ray scattering (SAXS). The first method involves shadowing of crystals with evaporated metal and measurement of the width of the shadows. We found $d = 9.5 \text{ nm} \pm 1.2 \text{ nm}$. The spread in the results is probably a consequence of irregularities in the surface of the electron

microscope grid, such as local tilt and steps.

For the SAXS-measurements, the crystals were sedimented and dried to form oriented mats (24). The periodicity perpendicular to the direction of sedimentation corresponds to the crystal thickness. Because the thickness is of the order of 10 nm, it can only be determined by X-ray diffraction when very small scattering angles are measured. Using a Kratky camera, d was found to be 9.6 nm $\pm$ 0.5 nm, in excellent agreement with the electron microscopy results. This value is smaller than those found by Roe et al. (3), in accordance with the general finding that thicker crystals are formed at higher temperatures.

The density of the crystals was obtained using a helium powder pycnometer (Micromeritics Auto Pycnometer 1320). This dry method is to be preferred over determinations involving suspended lamellae (eg. flotation techniques) because of the large surface/volume ratio of the solid. In a liquid environment solid/liquid interactions become relatively important and erroneous densities are found (25). Crystals were dried from a suspension in ethanol by evaporation in a rotating film apparatus and, subsequently, in a vacuum oven. Each sample was measured twice, first after drying at 50 ^{o}C and a second time after drying at 120 ^{o}C: both times the density was 1.37 g/cc. Thus any measurable effect of gas bubbles entrapped between the aggregated lamellae was absent. From the densities of amorphous and crystalline POM (1.25 g/cc and 1.49 g/cc, respectively (4)) the estimated crystalline content of single crystals is 50 %. This is surprisingly low when we consider the regular structure and smooth surface. However, similar results have been found in the literature for polyethylene (26), and recently also for POM (27).

From the crystalline content the thickness of the amorphous and crystalline layers of a single crystal are estimated to be 2.6 nm and 4.4 nm, respectively. By analyzing higher order reflections in SAXS measurements on POM crystals, Varnell et al. (24) could give an independent estimate of the amorphous layer thickness: for crystals of 9.7 nm overall thickness they arrived at 1.8 nm. The discrepancy with density measurements may be a consequence of different crystallization conditions: they crystallized POM from o-dichlorobenzene at 139 ^{o}C. Alternatively, with SAXS the boundary between the amorphous- and crystalline phases in a crystal could be situated at a different

position than would follow from density measurements. Roe et al. (3) used also 1.37 g/cc for the density, but they do not give any details about the determination.

From eq [1], the specific surface area is calculated to be 150 m^2/g. This result was not confirmed by nitrogen adsorption on freeze dried crystals: BET-analysis of the isotherm (measured on a Carlo Erba Sorptomatic 1800) yields a value of 30 m^2/g. The difference can only be explained if aggregation renders 80 % of the fold-planes inaccessible to nitrogen. Roe et al. (3) suggest a specific reason for the difference between geometric and accessible surface. As discussed above, in single crystal preparations often multilayer crystals are formed as a consequence of lattice imperfections, giving rise to spiral growth (14,28). An example was given in fig. 3. It looks as if successive layers are in direct contact, resulting in a diminished surface area available for adsorption. However, it should be remembered that fig. 3 exhibits a dried crystal, and in fact the only connection between the various layers is at the center of the pyramid. Apart from this connection each layer is a single crystal in itself. Under a light microscope, structures like the one shown in fig. 3 have often been observed, the layers splaying widely apart (29). Therefore, we do not think that it is justified to invoke the occurrence of spiral growth as the sole explanation for the difference between geometric and BET surface area. Rather, this difference should be understood as a consequence of aggregation that might occur between any pair of lamellae, and not just between two successive layers in a multilayer crystal.

Of course, aggregation may be a consequence of freeze drying. Then the BET-surface is not representative for crystals suspended in water. The "wet" surface area of suspended adsorbents is in general determined from the adsorption isotherm of some standard compound. Ideally, the adsorption plateau corresponds to a complete monolayer and the specific surface area then follows directly from the known molecular cross-section of the adsorbate. However, Roe et al. (3) did not succeed in finding a suitable low molecular weight substance that adsorbs in significant amounts on POM crystals. They tested stearic acid, methylene blue and p-nitrophenol. We obtained the same negative result for methylene blue and p-nitrophenol (in water at pH 3, where the

molecule is neutral, and in hexane). Also congo red, t-butyl ammonium iodide and 2,4-dichloro phenoxy acetic acid (2,4D) did not adsorb in appreciable amounts. We found, however, that polyoxyethylated nonyl phenols ("Synperonic" NPn, ex ICI) adsorb well on POM crystals. These nonionic surfactants (abbreviated as NPn) have the structure C_9H_{19}-phe-O-$(C_2H_5O)_n$-H, and are commercially available. NPn from various sources has been used before in adsorption experiments on carbon black (30,31), calcium carbonate (32) and on silica (31,33,34,35).

Adsorption isotherms of three NPn homologues (n=15,20,30) on POM-crystals were measured by the depletion technique. In a centrifuge tube the POM suspension was mixed with NPn solution and subsequently gently agitated on a rotating wheel until equilibrium was established (ca. 15 h). The adsorbent was separated from the supernatant by centrifuging. Concentrations were determined spectrofotometrically, using the extinction at 278 nm. It was found that the calibration curves of extinction vs. concentration always consisted of two straight lines with an intersection point at the CMC (CMC values were taken from the literature (32,36)). The different slopes reflect the different extinction coefficients of NPn molecules free in solution and those incorporated in a micel (37).

	Silica		POM	
	Γ_{max} (μmol/g)	m	Γ_{max} (μmol/g)	m
NP15	> 130	-	130.0 $\pm$ 2.0	15
NP20	82.0 $\pm$ 1.5	5	77.5 $\pm$ 1.8	27
NP30	47.2 $\pm$ 1.0	9	42.9 $\pm$ 0.8	21

Table I: Plateau values of the adsorption isotherms of NPn (fig. 5) on aerosil Ox-50 and on POM. The standard deviation of the mean, and the number of points m on which it is based, are indicated.

Fig 5 gives the adsorption isotherms and in table I the plateau values are summarized. As a reference, corresponding results for the same NPn batches on silica (aerosil Ox-50) are included (38). We will

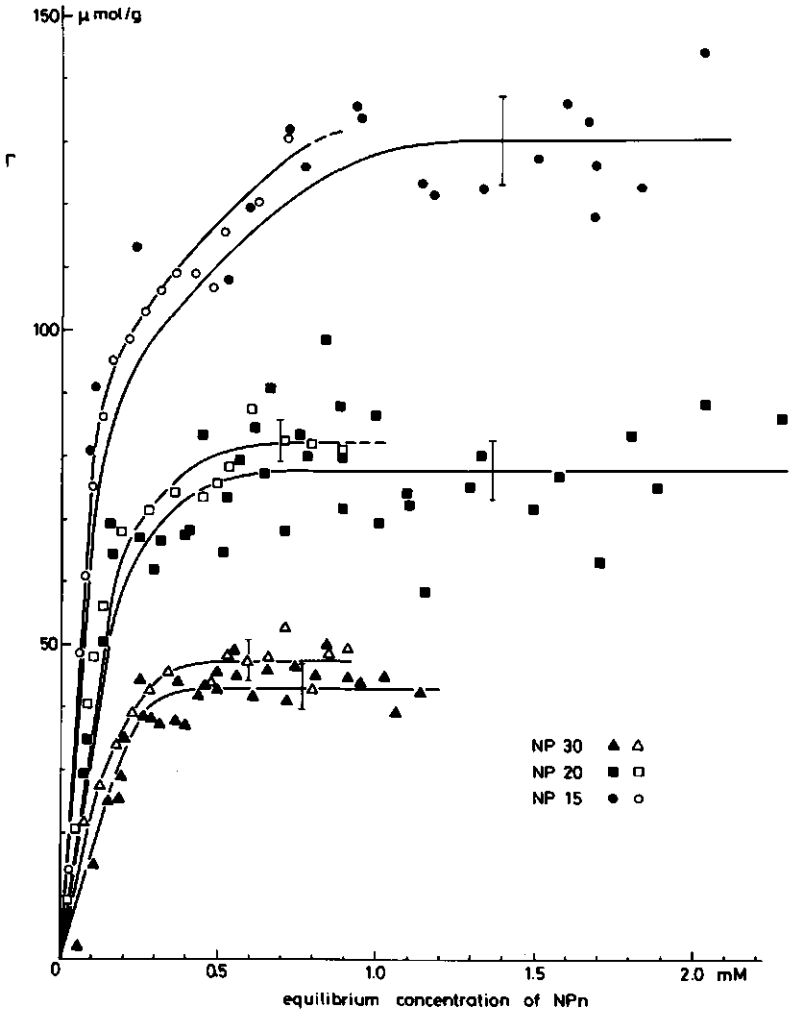

Figure 5: Adsorption of NPn (n = 15, 20, 30) on POM crystals (filled symbols) and on aerosil Ox-50 (open symbols). The plateau levels drawn correspond to the average of the adsorbed amounts at equilibrium concentrations above 0.3 mM (NP30), 0.5 mM (NP20) and 0.7 mM (NP15), respectively. The error bars indicate the standard deviation in the plateau values.

interpret the isotherm data taking into account the results by Seng and

Sell (34), who investigated the adsorption of NPn on silica (aerosil 200) and on some modified silicas. The latter were prepared from aerosil 200 by esterification of the surface silanol groups with various hydrophobic compounds. The adsorbed amount, and its variation with the length of the ethylene-oxide chain, n, were found to depend strongly upon the polarity of the surface. Nitrobenzyl aerosil, the most polar of the substituted aerosils, closely resembled unmodified aerosil in this respect. For the various NPn samples, the adsorbed amount was found to be about the same on both silicas. Moreover, the molecular cross-section turned out to increase linearly with n. From this result the authors conclude that on nitrobenzyl aerosil and on unmodified aerosil the adsorption is determined by interactions between the polar surface and the relatively polar ethylene oxide moiety of the adsorbate. This conclusion is confirmed by the observation (38) that latex suspensions are stabilized by NPn adsorption layers, indicating adsorption via the nonyl group, whereas aerosil suspensions are not. It seems justified for adsorption of NPn on POM, to postulate a mechanism which is similar to that for adsorption of NPn on aerosil, since in the adsorbate and in both surfaces ether-like groups are present. The close analogy between isotherms on POM crystals and on aerosil Ox-50 (fig. 5 and table I) supports this conclusion. Also, on POM and on silica the plateau adsorption varies in the same manner with n, and the shape of the isotherms on POM and on silica is essentially identical. Therefore, we assume that the molecular cross-section of NPn on POM equals that on unmodified (or nitrobenzyl substituted) aerosil. This assumption allows calculation of the specific surface area of the POM crystals from the adsorption plateaus in table I, provided the surface area of aerosil Ox-50 is known. By nitrogen adsorption this was found to be 60 m^2/g (38). For silica it is generally accepted, that in water this same surface area is exposed (31,33,34,35). Then the "wet" specific surface area of POM crystals is also almost 60 m^2/g. Obviously, in water aggregation is less than for freeze dried crystals, but still 60 % of the surface is not accessible for the adsorbing molecules.

The crystal surface is expected to consist of stretches of ether groups in a folded conformation, and should thus be uncharged. This was checked by electrokinetic measurements on a plug of crystals prepared by repeated centrifugation. The surface charge varied somewhat with pH and

ionic strength but was always negligibly small (between + 0.10 and - 0.17 $\mu C/cm^2$).

Discussion

A prerequisite for any substrate to be useful in systematic adsorption studies is the availability of a method to produce large amounts in a reproducible way. So far, we prepared and characterized two batches. The reproducibility of the method was established by the fact that for these batches both the electron microscopic thickness and the surface area as determined by NPn adsorption were almost the same.

The nature of the POM single crystal surface may be assessed in a qualitative way. The surface consists of folded $[CH_2\text{-}O]_n$ chains and is essentially uncharged. The occurrence of flotation when sufficient air is present in the solution indicates that the surface is not readily wetted by water, i.e. it is hydrophobic, as would be expected from its ether-like chemical composition. Finally, it was observed that the POM surface behaves like the surfaces of silica and nitrobenzyl silica (34) in adsorption experiments with various nonylphenols from aqueous solution. This indicates that the surface, though hydrophobic, is still rather polar.

In the specific surface area of POM crystals obtained with different methods large discrepancies were found. As discussed before, these are due to varying degrees of association of the crystals in suspension and in the dry state. For other adsorbents, such as AgI sols and suspensions, the surface areas found with BET and adsorption from solution are in general equal to the geometric surface area (39) (significantly larger values are found from capacitance and negative adsorption data, but such measurements are impossible for POM crystals). The difference in this respect between AgI and POM, both hydrophobic but still rather polar, is in our opinion a consequence of the fact that AgI forms rigid particles that usually carry some surface charge, whereas the flexible POM lamellae are essentially uncharged. In the absence of charge repulsion POM crystals aggregate more easily and large portions of the surface may be involved in the association, because of the flexibility of the lamellae. In interpreting adsorption from solution

the surface area determined by NPn adsorption is to be preferred over the geometric and the BET surface area. We do not expect that the degree of association of suspended crystals depends on the type and concentration of the adsorbate present. If that were the case, the adsorption isotherms with NPn on POM would not have followed so closely the trends observed with silica (fig. 5 and table I).

In our simple procedure for adsorption measurements by depletion a complication arises from the fact that POM suspensions sediment. Therefore, samples were taken while the suspension was homogenized by stirring, by means of a pipet immersed to a constant depth. Along with each isotherm one or two separate samples were dried and weighed in order to check the amount of adsorbent present in a sample. The dry weight found in this way was always accurate to ca. 2 % of the average over all determinations. Therefore, for each point of an isotherm the same amount of adsorbent may be assumed to be present. This procedure can hardly be improved by measuring, after adsorption, the weight of adsorbent for each point of the isotherm. A centrifuge tube contains only 10 mg of POM and an accurate determination of such a small amount is not possible in the presence of solutes.

As an illustration of the potentialities and limitations of POM single crystals as an adsorbent we discuss some preliminary adsorption results. As mentioned above, many substances of low molecular weight, whether charged (methylene blue, stearic acid) or uncharged (p-nitrophenol from water at pH 3, or from hexane) do not adsorb in appreciable amounts. Presumably, this is a consequence of a low affinity for the surface. Compounds of higher molecular weight do adsorb, as illustrated above by the NPn-results. Roe et al. (3) measured the adsorption of polystyrene (from cyclohexane) and of various proteins (from water). In our laboratory, we carried out some preliminary experiments with albumin (40) and sodium polystyrene sulfonate (NaPSS) from saline solutions. It can be concluded that high molecular weight substances adsorb on POM due to the large number of contacts between these adsorbate molecules and the surface. However, though adsorption of albumin (40) and NP30 is complete within 20 h, we found that for NaPSS it takes over 100 h to reach adsorption equilibrium. This time dependence is probably related to reorientation effects, not only of the adsorbate, but also of the POM crystals. The

polymeric lamellae are flexible enough to adjust to newly forming adsorption layers, but their lateral size (ca. 1 μm) and the fact that these lamellae are two-dimensional structures (which are sometimes also partially interconnected, see the discussion of fig. 3) would make this a slow process. Apparently, only for NaPSS such reorientation effects play a dominant role in adsorption kinetics. This may be a consequence of the fact that NaPSS forms rather thick adsorption layers, necessitating more extensive reorientation of the substrate POM lamellae upon adsorption. Takahashi et al. (41) report values for the thickness of adsorption layers of NaPSS that range between 20 nm and 80 nm. Albumin, on the other hand, is found to form compact layers of only 2 nm thickness (42,43) and also for NPn the adsorption layer is expected to be rather thin.

It may be concluded that single crystals of POM can be prepared reproducibly in large amounts, and that adsorption measurements from aqueous solution are feasible for compounds of not too low molecular weight. The features that make POM crystals attractive as a model adsorbent are the homogeneous, uncharged surface and the relatively large surface area per gram.

Acknowledgements

Thanks are due to Mr. J. Groenewegen (department of Virology, Agricultural University, Wageningen) for assistence with electron microscopy, and to Mr. A.M.L. Hustings (Dutch State Mines) and Mr. J.A.H.M. Moonen (University of Utrecht) for performing the density and SAXS measurements, respectively. We appreciate the discussions with Mr. Th. van den Boomgaard about his, as yet, unpublished results. The cooperation of Mr. A.J. Korteweg (BET measurements) and of Mr. A.J. van der Linde (streaming potential experiments) is gratefully acknowledged.

References

1. Geil, P.H., "Polymer Single Crystals," p. 79. Robert E. Krieger Publishing Company, Huntington, New York, 1973.
2. Wunderlich, B., "Macromolecular Physics," Vol. 1, p. 232, Academic Press, New York, 1973.
3. Roe, R.J., Shastri, R., and Wille, W., J. Colloid Interface Sci. 84, 346 (1981).
4. Gaur, U., and Wunderlich, B., J. Phys. Chem. Ref. Data 10, 1001 (1981).
5. Basset, D.C., and Keller, A., Phil. Mag. 7, 1553 (1962).
6. Blundell, D.J., and Keller, A., J. Macromol. Sci.-Phys. B2, 301, 337 (1968).
7. Khoury, F., and Barnes, J.D., J. Res. Nat. Bur. Stand. 87A, 95 (1974).
8. Ref. 1, p. 9.
9. Ref. 2, p. 165.
10. Ref. 1, ch. I.4.
11. Ref. 2, ch. II.4.
12. Ref. 1, p. 487.
13. Ref. 2, p. 208.
14. Ref. 2, p. 259.
15. Ref. 2, p. 299.
16. Ref. 1, p. 88; Ref. 2, p. 194.
17. Ref. 1, ch. V.
18. Wunderlich, B., "Macromolecular Physics," Vol. 2, ch. VII, Academic Press, New York, 1976.
19. Manufacturer's information.
20. Ref. 18, p. 207.
21. Ref. 18, p. 91.
22. Ref. 18, p. 81.
23. Fuchs, O., and Suhr, H.-H., in "Polymer Handbook" (J. Brandrup and E.H. Immergut,Eds.), 2nd Ed., p. IV-241, Wiley-Interscience, New York, 1975.
24. Varnell, W.D., Runt, J.P., and Harrison, I.R., J. Polym. Sci. Polym. Phys. Ed. 19, 1923 (1981).
25. Ref. 2, table IV.2.

26. Ref. 2, p. 386.
27. Shimomura, M., and Iguchi, M., Polymer 23, 509 (1982).
28. Ref. 1, p. 153.
29. Ref. 1, p. 160; Ref. 2, p. 264.
30. Abe, R., and Kuno, H., Kolloid-Z. Z. Polymere 181, 70 (1961).
31. Aston, J.R., Furlong, D.N., Grieser, F., Scales, P.J., and Warr, G.G., in "Adsorption at the gas-solid and liquid-solid interface" (J. Rouquerol and K.S.W. Sing,Eds.), p. 97, Elsevier Scientific Publishing Company, Amsterdam, 1982.
32. Akers, R.J., and Riley, P.W., J. Colloid Interface Sci. 48, 162 (1974).
33. Rupprecht, H., and Liebl, H., Kolloid-Z. Z. Polymere 239, 685 (1970).
34. Seng, H.P., and Sell, P.J., Tenside Detergents 14, 1 (1977).
35. Furlong, D.N., and Aston, J.R., Colloids and Surfaces 4, 121 (1982).
36. Hsiao, L., Dunning, H.N., and Lorenz, P.B., J. Phys. Chem. 60, 657 (1956).
37. Luck, W., in "Proceedings of the 3rd Int. Congress on Surface Activity," Vol. 1, p. 264, Cologne, 1960.
38. Van den Boomgaard, Thesis Agricultural University, Wageningen, in preparation.
39. Koopal, L.K., Thesis Agricultural University Wageningen, 1978.
40. Nowicka, G., personal communication.
41. Takahashi, A., Kawaguchi, M. and Hayashi, K., ACS Symposium "Colloidal Particles: Polymer Adsorption and Steric Stabilization," Washington, 1983. ACS Symposium Series, 240, 39 (1984).
42. Cuypers, P.A., Hermens, W.Th., and Hemker, H.C., Anal. Biochem. 84, 56 (1978).
43. Uzgiris, E.E., and Fromageot, H.P.M., Biopolymers 15, 257 (1976).

CHAPTER 3

Polystyrene Sulfonate: Chemical and Physical Characterization

Introduction

In studies on polyelectrolyte solution properties, polystyrene sulfonate (PSS) has been used most widely as a model substance. The sulfonate group is strong (1) and therefore the charge density along the chain is independent of pH and counterion concentration. Specific monomer-monomer interactions are absent. PSS may thus be described as a random coil, a wormlike chain or a rigid rod, depending upon the amount of indifferent electrolyte added. Moreover, PSS concentrations are conveniently determined by UV absorption because in each monomeric unit an aromatic chromophore is present.

Generally, sulfonated aromates are prepared by electrophilic substitution with concentrated sulfuric acid (2). Analogously, PSS may be obtained by sulfonation of the corresponding polystyrene. The dispersion index of the product is, in principle, the same as that of the parent PSS. However, the reaction must be highly specific because the monosulfonated monomeric units cannot be separated from unreacted, doubly substituted or cross-linked monomers. Obviously, even one interchain cross-link per macromolecule would double the molecular weight. Carrol and Eisenberg (3) describe a procedure to sulfonate polystyrene exclusively in the p-position, avoiding secondary reactions. To this end, finely dispersed polystyrene powder is mixed rapidly at room temperature with 100 % sulfuric acid in the presence of a fairly high concentration of silver ion, acting as a catalyst. The reaction is complete within 15 minutes, and the PSS is then isolated from the reaction mixture by dilution and dialysis. It is essential now to neutralize the poly-acid, for instance by titration with NaOH, because the acid form is not stable with respect to chemical degradation. This problem is mentioned by several authors (3,4) but the nature of the degradation reactions has not been clarified. Probably the formation of

sulfone bridges (R_x-SO_2-R_y), a well-known side reaction in the sulfonation of polymers (5), plays a role here. Only 0.1 % of cross-links makes the polyelectrolyte completely insoluble.

Virtually homodisperse PSS samples are commercially available. This is important in model studies involving such techniques as viscosity measurement and light scattering, and also in adsorption experiments. Our interest is mainly in this latter aspect, and for that purpose homodisperse material is essential. Cohen Stuart et al. (6) pointed out that the adsorption behaviour of polydisperse polymer is markedly different from that of homodisperse samples. When chains of different length are present, the longer ones adsorb preferentially and the measured isotherms are not of the high affinity type that is predicted for polymer adsorption.

We used ten samples of homodisperse NaPSS, obtained from Pressure Chemical Co., produced by sulfonation of homodisperse polystyrene standards. The manufacturer does not give any further details, but probably a procedure was followed analogous to that of Carrol and Eisenberg (3), described above. The molecular weights, calculated from those of the parent polystyrenes by assuming 100 % sulfonation, are listed in table I along with the dispersion indices as specified by the manufacturer (7). If no side-reactions occur, these should correspond to those of the parent polystyrenes. The latter are prepared by anionic polymerization (8) resulting ideally in a Poisson distribution of chain lengths. For such distributions, the M_w/M_n ratios are much smaller than the values specified in table I, however, and even become unity for molecular weights larger than 88 kg/mole. For some samples the manufacturer specifies the degree of sulfonation but, unfortunately, most of the information does not apply to the samples we obtained. The values range between 70 % and 90 % (7). This is remarkably low when we consider the results of Carrol and Eisenberg (3), who conclude from elemental analysis that their sulfonation procedure leads to 100 % substitution. These authors also find that PSS samples may contain over 10 % of water by weight. The analysis by the manufacturer only involved determination of the sulfur content in a weighted sample, and probably the presence of hydration water was overlooked. Therefore we checked the degree of sulfonation by analyzing all samples for two elements, carbon and hydrogen. From these two data

both the water content and the sulfur content are easily calculated. The procedure and results are discussed in the following section.

Specifications			Experimental results				
M kg/mole	lot no.	disp. index	hydr. numb.	degr. sulf.	ϵ_{263} $M^{-1}cm^{-1}$	ϵ_{226} $M^{-1}cm^{-1}$	[η] g/g
1.6	23	1.25	1.8	0.94	481.6	13,560	3.11
4.0	18	1.10	2.1	1.04	471.2	12,609	3.95
6.5	27	1.10	2.7	0.96	470.8	12,637	4.10
16	20 d	1.10	2.2	0.86	446.0	11,620	8.43
idem	idem	"	2.9	0.85	-	-	-
31	* d	1.10	1.9	0.94	425.0	11,408	16.32
88	* d	1.10	2.0	1.01	427.7	11,612	30.09
177	26 d	1.10	2.1	0.90	426.7	11,668	51.01
idem	idem	"	1.9	0.97	-	-	-
354	* d	1.10	1.6	1.03	414.1	11,610	106.73
690	* d	1.10	1.8	1.00	423.7	11,527	163.11
1060	* d	1.10	2.2	0.96	473.7	12.306	121.03
repl	* d	1.10	-	-	-	-	130.27

Table I: Properties of eleven polystyrene sulfonate samples. The first column gives the molecular weight (to the exclusion of the counterion), the second column the lotnumber as given by the manufacturer. Unspecified lotnumbers are indicated by *, and if the sample was obtained in dialyzed form, this is denoted by d. Underlined numbers are used when the results point to systematic deviations beyond experimental error.

Subsequently, we measured for all samples the molar extinction coefficients at two absorption maxima. The determination involved complexometric titration of the PSS solutions with polylysine, in order to find the concentration. Due to the presence of variable amounts of hydration water, weighing does not give the correct amount of polyelectrolyte in solution. In this way extinction coefficients are obtained that may serve as a standard for PSS concentration measurements by UV absorption. Also, the results provide a second means to characterize the PSS samples, and are expected to reflect variations, if any, in the degree of sulfonation.

Finally, we characterized PSS-solutions viscosimetrically. According to Mark-Houwink's relation a linear relationship between log $[\eta]$ and log M is expected, and deviations would indicate chemical or physical inhomogeneity in the respective samples.

Elemental analysis

Analysis of the PSS samples for carbon and hydrogen was carried out by combustion of a few milligrams in an atmosphere of pure O_2, and measuring the amounts of CO_2 and H_2O released. The results are correlated with the degree of sulfonation y and with the hydration number x per monomeric unit, for the structure of which we may write:

$$C_8H_{8-y}(SO_3)_yNa_y(H_2O)_x \qquad [1]$$

NaPSS is hygroscopic, and consequently x may depend upon storage conditions. On the other hand, y is a constant for a particular sample. From the molecular formula and the appropriate atomic weights, the hydrogen and carbon content fH and fC can be expressed as:

$$fH = \frac{1.0079(8-y) + 2.0158x}{104.1512 + 18.1108x + 102.0401y} \qquad [2a]$$

$$fC = \frac{96.088}{104.1512 + 18.1108x + 102.0401y} \qquad [2b]$$

Values for the hydration number x and the degree of sulfonation y, calculated from the experimental quantities fH and fC, are given in table I. The degree of sulfonation of most samples does not deviate significantly from unity. This confirms the results of Koene and Mandel (9), who worked with NaPSS from the same manufacturer. Only for M = 16 kg/mole did we find a degree of sulfonation significantly less than unity. It is obvious that each sample contains around 20 % of hydration water (w/w), enough to explain the low degrees of sulfonation reported by the manufacturer.

Extinction coefficient

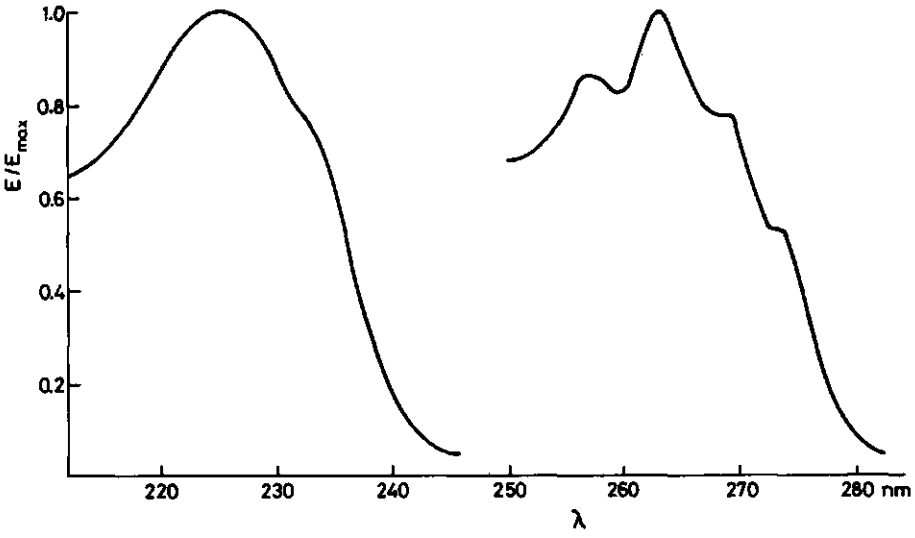

Figure 1: Normalized UV absorption spectrum for PSS in water. For each absorption band, the extinction E is scaled with the value of the corresponding absorbtion maximum E_{max}.

In the absorption spectrum of PSS in water two bands can be distinguished (Fig. 1), one around 226 nm and one around 263 nm. The first is of fairly high intensity and corresponds to the 200 nm band of the benzene ring (10). The shift to longer wavelength is due to extension of the conjugated π-electron system by sulfonate substitution. The second band is of low intensity and shows clearly the composite structure of the so-called benzenoid band characteristic of benzene derivatives. In pure benzene, this band occurs around 260 nm (10). Apparently, the position of this band is only slightly shifted by the presence of the sulfonate group. In principle, the extinction per monomole should not depend upon the molecular weight of the PSS. Therefore, comparing the monomolar extinction coefficients of all samples at 226 nm and 263 nm, respectively, provides a check upon the

chemical and physical homogeneity of each sample. Determination of the extinction of a PSS solution is straightforward. However, in order to calculate the monomolar extinction coefficient one needs the concentration of polymer without hydration water. This is most commonly obtained either by weighing an exhaustively dried sample (11,12), or by determination of the residual water content at the moment the solution is prepared (3,9,13). With the first method complete removal of all hydration water is never certain. Methods to measure the water content of a sample (IR and elemental analysis) are not expected to be very accurate. An alternative method to determine the concentration is acidimetric titration, after conversion of the NaPSS into the acid form (14,15). For PSS this method is not reliable because of the above mentioned instability of the acid form. Nevertheless, titration methods offer the fundamental advantage of being independent of the presence of hydration water. Therefore, we determined the concentration of PSS solutions by complexometric titration with a solution of polylysine (M = 40 kg/mole; ex Sigma), a polycation at neutral pH. Titration of oppositely charged polymers is known to result in stoichiometric complexation of the charged groups (16,17) and this method is thus well suited to determine the amount of sulfonated monomeric units in a PSS solution. The concentration of the polylysine solution was obtained by titrating the counterion, Br^-, with $AgNO_3$ solution of known concentration. In order to assure that all polylysine was in the bromide form, the solution was first dialyzed against 0.2 M NaBr and then extensively against doubly deionized water. However, when undialyzed polylysine was used the results were not significantly different.

The extinction coefficients are listed in table I. Only with five samples (M = 31, 88, 177, 354 and 690 kg/mole) are the results, within experimental error, invariant with molecular weight. By averaging the values for these samples we find $\varepsilon_{226} = 1.16 \pm 0.01 * 10^4\ M^{-1}cm^{-1}$ and $\varepsilon_{263} = 423 \pm 5\ M^{-1}cm^{-1}$, respectively. From fig. 5 in the paper by Carrol and Eisenberg (3), about the same value can be deduced for ε_{226} (= 11,900). In most cases however, the values reported for ε_{226} (4) and for ε_{263} (3,12,15) are between 6 % and 12 % less than our results. This indicates that either the water content of the PSS sample was underestimated, when the PSS concentration was obtained through weighing

(3,12), or chemical modification had occurred, in case of titration of HPSS (15).

As mentioned above, the sample with M = 16 kg/mole is sulfonated to a degree significantly less than 100 %, and this is well in line with the magnitude of the extinction coefficient. With the titration method only the concentration of sulfonated monomers is measured, and only these monomers absorb radiation of wavelength 226 nm (the corresponding absorption band of unsulfonated monomer lies below 200 nm). Therefore, ε_{226} is not expected to differ from the value found for 100 % sulfonated PSS. We already mentioned that the position of the absorption band around 260 nm is only slightly influenced by the presence of a sulfonate group. Thus both sulfonated and unsulfonated monomers will attribute to the extinction at 263 nm, the former relatively more than the latter. Consequently, the experimental extinction coefficient at this wavelength is expected to increase with decreasing degree of sulfonation, but less than proportional, in agreement with our results.

For the four remaining samples (M = 1.6, 4, 6.5 and 1060 kg/mole) erratically high extinction coefficients are found at both wavelengths. This may be due to either experimental error (e.g., in the titrations) or some imperfection in the samples. They could be chemically inhomogeneous (e.g., as a result of cross-linking), or heterodisperse with respect to chainlength. When in a sample cross-links are present, it is conceivable that complexation with polylysine is no longer stoichiometric and consequently the PSS concentration is underestimated. The presence of a low M fraction (monomers, dimers, trimers) which are possibly not completely bound by the polylysine, is expected to have the same effect. In this context we mention that the smaller three samples can not be dialyzed because the molecular weights are well below the cut-off values of most dialysis membranes.

Viscosity of polystyrene sulfonate solutions

The intrinsic viscosity of a polymer solution is determined by the molecular weight of the polymer and by the interaction with the solvent. When the latter is kept constant, the relation between $[\eta]$ en M can be expressed by the Mark-Houwink relation:

$$[\eta] = K \cdot M^a \qquad [3]$$

where K and a are constants for a given polymer and solvent. According to this equation a plot of log $[\eta]$ vs. log M should result in a straight line with slope a and intercept log K.

Viscosity measurements were carried out with an Ubbelohde viscometer suspended in a waterbath at 20.0 °C. Solutions were made up in 0.5 M NaCl in order to suppress effects of variations in the counterion concentration upon varying the PSS concentration. The results are summarized in table I and graphically presented in Fig. 2.

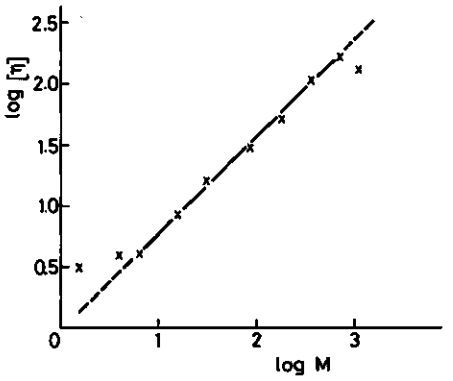

Figure 2: Mark-Houwink plot (eq. [3]) of intrinsic viscosities for NaPSS in 0.5 M NaCl at 20.0 °C: log $[\eta]$ vs. log M ($[\eta]$ in g/g and M in kg/mole). From the linear part of the curve we find K = 1.087 g/g and a = 0.764.

The intrinsic viscosities of seven samples conform to the relationship predicted by eq. [3], with K = 1.087 g/g and a = 0.764, but for the two shorter and for the highest chain length significant deviations are found. For the highest M we found no improvement with a substitute sample, received after communicating the initial result to the supplier. The deviations in $[\eta]$ are of the order of 25 % - 50 % and can not be caused by errors in the concentration determination. Moreover, the correlation with erratic extinction coefficients (viz. table I) indicates that some trivial explanation, such as wrong labelling of the flasks, does not account for the results either. As mentioned before, both heterodispersity and cross-linking could account for too high extinction coefficients, and the deviating intrinsic viscosities might be explained along the same lines. If we assume that

the samples are heterodisperse the measured viscosity could well be higher than predicted if a few very long chains were present (M = 1.6 and 4 kg/mole), but it could also be smaller if short chains dominate (M = 1060 kg/mole). In case of cross-linking, interchain cross-links are favoured when a sample contains many small molecules (M = 1.6 and 4 kg/mole) and intrachain cross-links will dominate when few large molecules are present (M = 1060 kg/mole). In the first case the intrinsic viscosity is larger than expected, in the second case it would be smaller.

Conclusions.

We characterized ten PSS samples of narrow molecular weight distribution with three different techniques, elemental analysis, extinction coefficient determination and viscometry, respectively. For the three lowest molecular weights and for the highest molecular weight sample, the results with two techniques raise doubts about the quality of the sample, whereas with M = 6.5 kg/mole only the extinction coefficients are found to be too high. We conclude that only the remaining five samples satisfactorily meet the high standards of chemical and physical homogeneity that polyelectrolyte model substances should conform to. For these samples the degree of sulfonation is 97.5 %, the extinction coefficients are $\varepsilon_{226} = 1.16 * 10^4\ M^{-1}cm^{-1}$ and $\varepsilon_{263} = 423\ M^{-1}cm^{-1}$, and the intrinsic viscosity conforms accurately to the Mark-Houwink relation in 0.5 M NaCl aqueous solution with K = 1.087 g/g and a = 0.764.

References

1. Roberts, J.D., Stewart, R., and Caserio, M.C., "Organic Chemistry", p. 527, W.A. Benjamin Inc., Menlo Park, California, 1971.
2. Ref. 1, p. 566.
3. Carrol, W.R., and Eisenberg, H., J. Polym. Sci.: Part A-2 4, 599 (1966).

4. Reddy, M., and Marinsky, J.A., J. Phys. Chem. 74, 3884 (1970).
5. Roth, H.H., Ind. Eng. Chem. 49, 1820 (1957).
6. Cohen Stuart, M.A., Scheutjens, J.M.H.M., and Fleer, G.J., J. Polym. Sci. Polym. Phys. Ed. 18, 559 (1980).
7. Product Information, Pressure Chemical Co.
8. Elias, H.-G., "Makromolekuele", p. 503 ff., Huethig & Wepf Verlag, Basel, 1972.
9. Koene, R.S., and Mandel, M., Macromolecules 16, 220 (1983).
10. Ref. 1, p. 554.
11. Caille, A., and Daoust, H., J. Polym. Sci.: . Symp. 45, 153 (1974).
12. Bloys-van Treslong, K., personal communication.
13. Tricot, M., and Houssier, C., Macromolecules 15, 854 (1982).
14. Oman, S., Makromol. Chem. 175, 2133 (1974).
15. Okubo, T., and Turro, N.J., J. Phys. Chem. 85, 4034 (1981).
16. Terayama, H., J. Polym. Sci. 8, 243 (1952).
17. Horn, D., Progr. Coll. Pol. Sci. 65, 251 (1978).

CHAPTER 4

Adsorption of Polystyrene Sulfonate on Polyoxymethylene Single Crystals at High Ionic Strength

Introduction

Adsorption of uncharged polymers has recently received much attention, both experimentally and theoretically. A clear picture for the structure of the adsorbed layer of uncharged polymers is now emerging. Several aspects have been reviewed by Fleer and Lyklema (1), who outlined the most important trends. In comparison, very little is known about the adsorption of polyelectrolytes. On the theoretical side, only two models have been published sofar. The first, a rather primitive one, is due to Hesselink (2), and recently Van der Schee (3) developed a more elaborate theory. In order to test these theories, experimental results with strong polyelectrolytes are most suitable. For this type of polyelectrolyte the degree of dissociation, and therefore the charge density along the chain, does not depend upon the local segment concentration. Unfortunately, experimental data on well-defined systems are very scarce. We found only five reports on relevant systems in the literature: polyvinyl pyridine on Vycor silicate glass in concentrated HCl solutions ($\geq$ 0.1 M) (4), positively charged polylysine on AgI (3,5), and polystyrene sulfonate (PSS) on platinum (6), on $CaCO_3$ (7) and on preheated silica (8). Only in the latter work was the effect of variations in polyelectrolyte concentration, ionic strength and molecular weight studied systematically. In all cases the surface was heterogeneous and, with the exception of preheated silica, highly charged, giving rise to a significant electrostatic component to the affinity between the segments and the surface. The presence of adsorbed polyelectrolyte may influence the surface charge by affecting specific adsorption of small ions. This effect hampers straightforward interpretation of experimental results.

In the present work we collect systematic data on polyelectrolyte adsorption in a well-defined model system. As the adsorbate we used PSS. This is a strong , flexible polyelectrolyte that can be obtained in the form of homodisperse samples. A low M_w/M_n ratio is important as heterodispersity may give rise to rounded isotherms (9). In the present paper we obtain also rounded isotherms. For our polyelectrolyte heterodispersity cannot be involved as a possible explanation. We explain the shape of the isotherms in terms of a weak adsorbent-adsorbate interaction. Single crystals of polyoxymethylene (POM) (10) were used as adsorbent. The hexagonal platelets have a homogeneous surface, consisting entirely of ether groups and carrying essentially no charge.

In the adsorption studies we varied the polyelectrolyte concentration, molecular weight and ionic strength. Elsewhere (11), a semi-quantitative comparison of the results with Van der Schee's theory will be given. Here, the results are compared with those on other systems and, in a qualitative way, with theoretical trends predicted by the models of Hesselink (2) and Van der Schee (3,8).

Substantial adsorption of PSS on POM crystals occurs only in the presence of high NaCl concentrations, and the measured isotherms are rounded. These features indicate weak surface-polyelectrolyte interaction. We also measured a few isotherms on hematite, possessing a a high-energetic, positively charged surface. With this adsorbent, adsorption readily occurs at low ionic strength, and high-affinity isotherms were obtained even at high salt concentration. Apparently, the affinity of the surface for the polyelectrolyte determines to a large extent both the amount adsorbed and the shape of the adsorption isotherm. In the case of POM, the affinity is only due to a weak non-electrostatic interaction, whereas for hematite it is made up of strong non-electrostatic and electrostatic contributions. Interpretation of literature data on various systems confirms that the magnitude of direct non-electrostatic surface-polyelectrolyte interactions determines the adsorption characteristics to a large extent. Not only the shape of the isotherms, but also the dependence of the adsorbed amount on molecular weight and on ionic strength appears to be correlated with the strength of these interactions.

Materials and methods

For the preparation of a large batch of POM crystals we followed a method described elsewhere (10). The specific surface area in water, determined from the adsorption plateau of the nonionic surfactant NP30 (C_9H_{19}-C_6H_4-O-$[C_2H_5O]_{30}$-H) (10), was 60 m^2/g.

The hematite sol was taken from a batch prepared by Breeuwsma and Lyklema (12). The specific surface area is 31 m^2/g and the pH of the point of zero charge 8.5. At neutral pH hematite forms a stable, positively charged sol.

M (kg/mole)	1.6†	4†	6.5†	16†	31	88	177	354	690	1060†

Table I: Molecular weights of NaPSS samples ex Pressure Chemical Co. The values indicated do not include the Na^+ counterion; unreliable samples (see text) are marked with †.

Ten samples of homodisperse NaPSS were obtained from Pressure Chemical Co. (table I). We characterized these samples by elemental analysis, UV spectroscopy and viscometry. The results have been reported extensively elsewhere (11). Here we repeat only the main conclusions. For all samples but one (M = 16 kg/mole) the degree of sulfonation did not differ significantly from 100 %. We measured the monomolar extinction coefficients ε of PSS solutions at 226 nm and 263 nm. These should be independent of chain length. However, for the four low molecular weight samples (M = 1.6, 4, 6.5 and 16 kg/mole) and for the highest molecular weight (M = 1060 kg/mole) ε deviated significantly from the values $\varepsilon_{226} = 1.16 * 10^4\ M^{-1}cm^{-1}$ and $\varepsilon_{263} = 423\ M^{-1}cm^{-1}$ found with the other samples. Intrinsic viscosities of all samples were measured in 0.5 M NaCl. From a plot of log $[\eta]$ vs. log M it appeared that the results with seven of these conform to the Mark-Houwink equation $[\eta] = K.M^a$ with K = 1.087 g/g and a = 0.764. Serious deviations from linearity were found with M = 1.6 kg/mole and 4 kg/mole ($[\eta]$ too high) and with M = 1060 kg/mole ($[\eta]$ considerably lower than expected). From these results we conclude that only five samples are sufficiently reliable. The other five (indicated in table I

by †) are to some extent suspect on account of deviating chemical, spectroscopic and/or viscometric properties. Although some adsorption experiments have been carried out with these samples, we do not trust the results fully.

The adsorbed amount was measured by the depletion method. Experiments were carried out at neutral pH, in centrifuge tubes that could be fitted with a screw-cap. The required amounts of water, NaCl solution, PSS solution and POM suspension or hematite sol were added by means of automatic pipettes. The accuracy of these pipettes is only of the order of 1 %, and even worse for the more viscous PSS stock solutions, the POM suspension and the hematite sol. In order to improve the accuracy, the tubes were weighed after each volumetric addition. In this way the added volumes are known with a maximum accuracy of the order of 0.5 µl, instead of 5 µl. Sampling of POM crystals was accomplished by withdrawing a volume from a stirred suspension. This was necessary because of the sedimentation of the crystals. The POM content did never differ more than 5 % from the average. Moreover, these deviations could mainly be attributed to weighing errors, because the amount of adsorbent in each sample was only 10 mg. Reproducible hematite samples could be taken without stirring because it is a stable sol. The dry weight of the POM suspension and the hematite sol were measured in separate experiments. Equilibration, at 20 °C on a rotating wheel, took one day with hematite and five days with POM as adsorbent. The adsorbent was separated from the supernatant by centrifugation. Initial and final PSS concentrations were determined from the extinction at 226 nm, and the adsorbed amount was calculated from the material balance.

For desorption experiments the sedimented POM crystals were resuspended in a solution of lower salt concentration. We assumed that the available surface area did not diminish appreciably by this procedure. The results presented in the following section (fig. 2) support this assumption. After equilibration for another five days and centrifugation, the concentration of PSS in the supernatant was measured again.

The apparent molar volume of the PSS monomer is given by Boyd (13) as 112 ml/monomole. Using this conversion factor we express all PSS concentrations in ppm (v/v).

Results and discussion

In this section we shall first discuss the time dependence and reversibility of PSS adsorption on POM crystals. Subsequently, adsorption isotherms are presented and compared with literature data. Then we consider in more detail the dependence of adsorption on the molecular weight of the adsorbate, and finally the ionic strength dependence of the adsorption is examined.

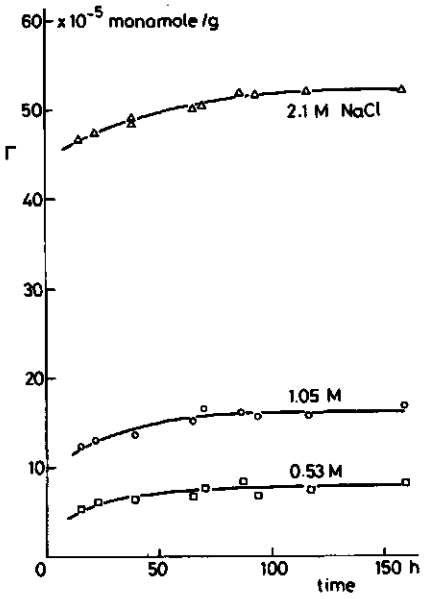

Figure 1: Adsorbed amount as a function of equilibration time, for PSS of molecular weight 177 kg/mole on POM, at three NaCl concentrations. The adsorbed amount is expressed in monomoles/g. The initial PSS concentrations and those finally left in solution were 37 ppm and 28 ppm at 0.53 M NaCl, 74 ppm and 55 ppm at 1.05 M NaCl and 148 ppm and 88 ppm at 2.1 M NaCl.

General

The first aspect to be studied in adsorption experiments is the time necessary to establish equilibrium. In fig. 1 we present the increase of the adsorbed amount with time for PSS of molecular weight 177 kg/mole, at three ionic strengths. In these experiments the initial concentration of PSS was kept constant for each curve. Adsorption increases during about 100 hrs; only at still longer times is a constant adsorption level reached. The slow establishment of

equilibrium may be due to slow reorientation of the flexible POM platelets upon formation of an adsorption layer. We discussed this matter before (10) and corroborated our conclusion by noting that PSS was found to form thick adsorption layers on platinum, between 20 nm and 80 nm (6). In order to accomodate such thick adsorption layers, extensive reorientation of the crystals would be required. NP30 and albumin, on the other hand, reach the maximum adsorption level on POM crystals within a day. This correlates with the fact that for NP30 thick adsorption layers are not expected, whereas the adsorbed layer thickness of albumin (on chromium and polystyrene, respectively) is about 2 nm (14,15). Apparently, the surface of crystals suspended in water is sufficiently exposed to allow the quick formation of such thin adsorption layers. We conclude that the slow progress of PSS adsorption on POM crystals may be explained in a physically realistic way. Clearly, it takes about 100 hrs. to establish adsorption equilibrium (fig. 1). We adopted a period of five days as the standard equilibration time in further adsorption experiments with POM crystals.

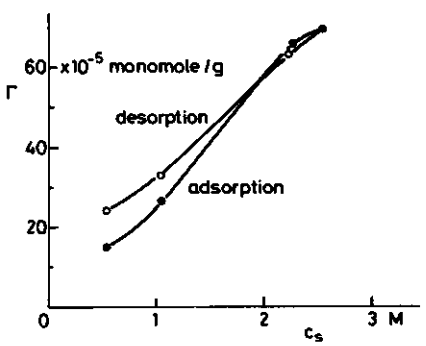

Figure 2: Desorption of PSS (M = 690 kg/mole) from POM crystals by decreasing the ionic strength. Initial equilibration occurred at 2.5 M NaCl, and desorption was accomplished by dilution with water or dilute NaCl solution. Results of direct adsorption experiments are given for comparison.

We checked the reversibility of the adsorption process in a desorption experiment with the sample of M = 690 kg/mole. After initial equilibration in the presence of 2.5 M NaCl, centrifugation and sampling of the supernatant, the crystals were resuspended in NaCl solutions of lower concentrations, viz., 0.5 M, 1.0 M and 2.2 M, respectively. In fig. 2 the adsorbed amount left on the crystals is compared with the results of direct adsorption experiments, both as a function of the salt concentration. At 2.2 M NaCl there is no significant difference,

whereas at the two lowest salt concentrations well over 80 % of the expected desorption actually takes place. The incomplete desorption at two NaCl concentrations might be a consequence of incomplete resuspension of the crystals. However, it could also be due to errors in the concentration determination. In adsorption experiments an error of 10 % in the adsorbed amount is often unavoidable. Desorption measurements are two-stage experiments, and therefore an error of 20 % in the amount desorbed from the surface is possible. Another complication may arise from the fact that desorption is a very slow process. Van der Schee (3) reports that for the AgI - polylysine system desorption takes well over five days, whereas adsorption equilibrium is established in one day. In view of these arguments we conclude that incomplete resuspension is not necessarily responsible for the difference between adsorption and desorption in fig. 2. The other explanations could well account for the incomplete desorption. In any case, the adsorption of PSS onto POM crystals may be considered to be virtually reversible.

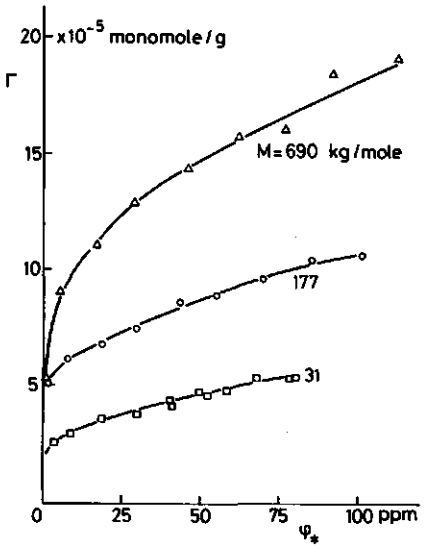

Figure 3: Adsorption isotherms of PSS on POM crystals, in the presence of 0.53 M NaCl, for three molecular weights.

Adsorption isotherms

In figs. 3, 4 and 5 we present adsorption isotherms of PSS on POM single crystals, for three molecular weights and at three different NaCl concentrations.

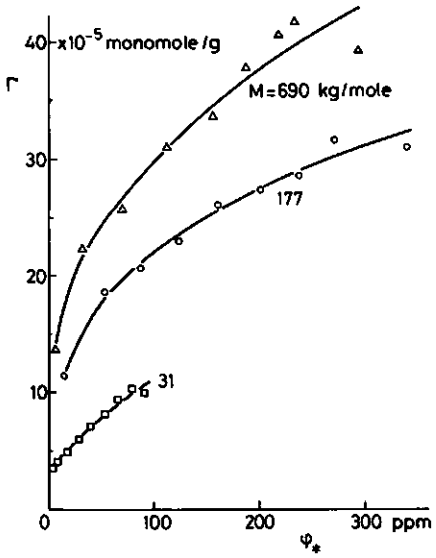

Figure 4: Adsorption isotherms at 1.04 M NaCl.

Note the different ordinate scales in these three figures. Obviously, the adsorbed amount not only increases with polyelectrolyte concentration and molecular weight, but also with ionic strength. Substantial adsorption does not occur for salt concentrations below 0.5 M, and all isotherms are of the low affinity type. Similar results were obtained by Marra et al. (8), for PSS (from the same supplier) on preheated silica, at comparable salt concentrations. Apparently, in both systems the adsorbent-adsorbate interaction is weak, and the mutual repulsion between charged segments at low salt concentrations effectively counteracts the adsorption forces. Significant adsorption occurs only when the segmental charges are effectively screened, at high salt concentration.

One would expect, therefore, that for systems with high affinity between segments and substrate the isotherms are less rounded. We checked this for the high-energetic, positively charged hematite surface. The adsorption of PSS (M = 690 kg/mole) was again measured in

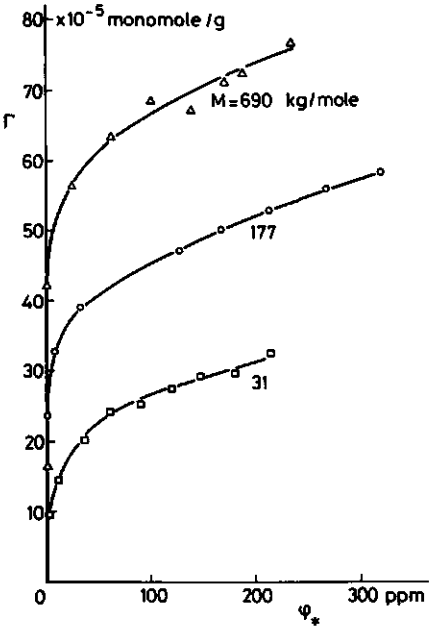

Figure 5: Adsorption isotherms at 2.18 M NaCl.

the presence of NaCl, at high and low ionic strength. In the latter case, the sum of NaCl and (initial) PSS concentration was kept constant along the isotherm (isoionic conditions). Keeping the concentration of NaCl constant at a level of 0.01 M would lead to variations in the ionic strength of up to 30 %, due to the contribution of the PSS itself. In fig. 6 two adsorption isotherms on hematite are given. In both cases high-affinity isotherms are obtained. The adsorbed amount is highest at 1 M NaCl. At this salt concentration, the non-electrostatic interaction probably dominates the affinity between surface and polyelectrolyte. On the other hand, at low ionic strength the electrostatic contribution becomes more important. Yet the adsorbed amount is lower than at high ionic strength, because diminished screening of the polyelectrolyte charges results in enhanced segment-segment repulsion. Apparently, strong adsorbent-adsorbate interactions, whether of electrostatic or of non-electrostatic nature, give rise to high-affinity isotherms. Literature data on polyelectrolyte adsorption onto high-energy surfaces, that carry a charge of opposite sign to that of the polyelectrolyte, corroborate the results found for hematite. Takahashi et al. (6) give adsorption isotherms for PSS (from the same source as ours) on platinum,

at NaCl concentrations as low as 0.1 M. Peyser and Ullmann report polyvinyl pyridine to adsorb readily onto silicate glass at the same ionic strength (0.1 M HCl) (4). Adsorption measurements by Van der Schee and Lyklema (5), with positively charged polylysine on negative AgI, were carried out at 0.01 M HNO_3, whereas Adam and Robb (7) adsorbed PSS (same manufacturer as ours) onto $CaCO_3$ from pure water. All these isotherms are of the high affinity type. Moreover, in line with our results on hematite (fig. 6), both on silicate glass (4) and on $CaCO_3$ (7) high-affinity isotherms are found at high ionic strength (0.9 M HCl and 0.5 M NaCl, respectively). This indicates that also in these systems the electrostatic contribution to the adsorbent-adsorbate affinity is augmented by a significant non-electrostatic term.

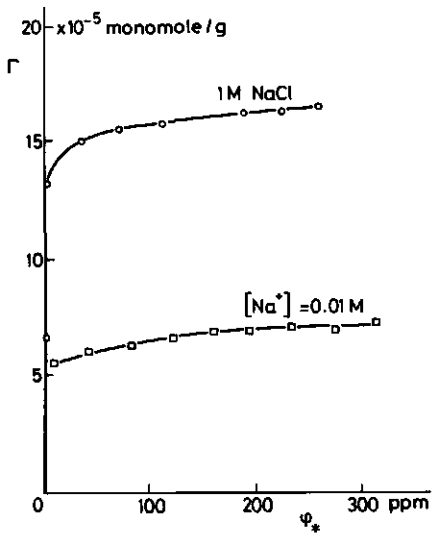

Figure 6: Adsorption isotherms of PSS (M = 690 kg/mole) on hematite, at ionic strength 0.01 M (pH = 6.2) and 1 M (pH = 6.6). The curve at 0.01 M applies to isoionic conditions (see text).

Theoretical calculations according to the models of Hesselink (2) and Van der Schee (3,8) confirm the important role of salt concentration, surface charge and adsorption energy in the adsorption process. However, theoretical isotherms are always of the high affinity type. The models do not predict the rather strong concentration dependence found for the POM-PSS system (fig. 3, 4, 5) and for the silica-PSS system (8).

An alternative explanation for rounded isotherms could possibly be related to heterodispersity of the adsorbate. It has been shown that for heterodisperse polymer the shape of the isotherm is influenced by the displacement of short chains by larger ones. Our PSS samples, though, are warranted as GPC standards. Therefore, heterodispersity does not seem a likely explanation for the low affinity isotherms found on POM and silica. Moreover, with heterodisperse polyelectrolyte high-affinity isotherms are sometimes also found. This was demonstrated by Adam and Robb (7) with a heterodisperse PSS sample on $CaCO_3$. Apparently, with polyelectrolytes high affinity isotherms are measured irrespective of the M_w/M_n ratio, provided the surface-adsorbate interaction is strong enough.

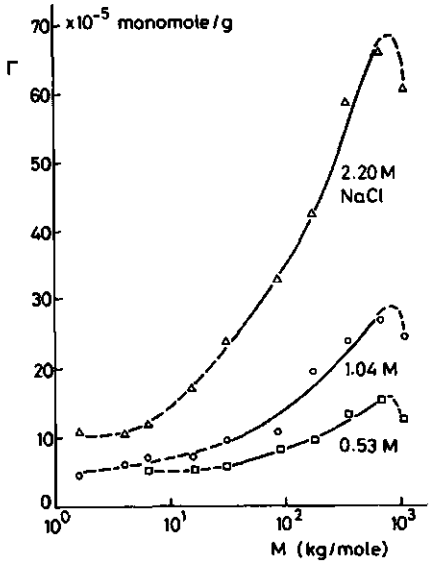

Figure 7: Adsorption of PSS on POM crystals, as a function of molecular weight, at three NaCl concentrations. The bulk concentration of PSS was 67 ppm. The dashed parts of the curves indicate results with samples that are not completely reliable (see text).

Adsorption as a function of molecular weight

In the discussion of figs. 3, 4 and 5 it was already mentioned that adsorption of PSS on POM crystals depends strongly on the molecular weight of the adsorbate. We checked this aspect in more detail and measured the adsorbed amount of ten PSS samples at a constant

equilibrium concentration (67 ppm) for three ionic strengths. The results are collected in fig. 7. The adsorbed amount at the required bulk concentration was determined by interpolation from five experimental points of the isotherm. Each point in fig. 7 represents the average of at least two, but usually more of such determinations. Fig. 7 also contains results for the PSS samples that were considered unreliable on the basis of characteristics measured with elemental analysis, UV spectroscopy and viscometry. The uncertain parts of the curves in fig. 7 are dashed. The unrealistic low intrinsic viscosity found for the sample of nominal M = 1060 kg/mole is reflected in the adsorbed amount which is, at any ionic strength, smaller than that for M = 690 kg/mole. For the samples with M between 31 kg/mole and 690 kg/mole the adsorbed amount increases roughly linearly with log M. For the lower molecular weights the dependency seems to be weaker. However, we do not want to ascribe too much importance to this last conclusion, in view of the uncertainties about these low M samples. Thus only data obtained with the five samples of M between 31 kg/mole and 690 kg/mole will permit straightforward interpretation. These results are confirmed by measurements of Marra et al. (8). For the adsorption of PSS (31 kg/mole $\leq$ M $\leq$ 354 kg/mole) on preheated silica, these authors also reported a strong, more or less linear dependence upon log M.

The strong increase of adsorption with molecular weight is another indication of a relatively weak adsorbent-adsorbate interaction. If energetic effects are small, the adsorption entropy determines the adsorption to a large extent, and many segments will be present in loops and tails. This is a well-known situation for uncharged polymers (1). Variations in adsorption entropy, due to differences in chain length, will then affect the adsorbed amount largely. Van der Schee and Lyklema (5) and Takahashi et al. (6) report data on the molecular weight dependence of the adsorption on AgI and platinum, respectively. From these results not only the high affinity character of the isotherms is evident, but also the near invariance of the results with molecular weight. The latter feature, in particular, indicates that the surface plays a dominant role in the adsorption process. Probably, in Van der Schee's and Takahashi's systems most segments of the adsorbed polymer chain are in direct contact with the adsorbent. In that case,

variations in adsorption entropy arising from differences in chain length would only be of secondary importance. The data of Adam and Robb (7) give no useful information on the molecular weight dependence of the adsorption on $CaCO_3$. The porosity of the adsorbent will favour adsorption of shorter molecules, that penetrate more easily into the narrow pores. Kinetic effects can therefore not be excluded.

When the surface is uncharged, Hesselink's theory (2) predicts a strong increase of adsorption with molecular weight. From the tabulated results an approximately linear dependence of adsorption on $\sqrt{M}$ can be inferred. Calculations by Marra et al. (8), using Van der Schee's model (3), yield a linear relationship between adsorbed amount and log M. Hence, both theories corroborate the strong dependence of adsorption on molecular weight that is experimentally obtained for uncharged, low-energy surfaces at high ionic strength. In effect, under these conditions the molecular weight dependence of polyelectrolyte adsorption theories resembles that of the parent models for uncharged polymers: Hesselink's theory is based on Hoeve's model, predicting a square root dependence of adsorption on chain length, and that of Van der Schee uses the Roe theory, giving approximately a linear relation between adsorbed amount and log M (1). With Van der Schee's model, the near-invariance of adsorption with molecular weight on high-energy surfaces that are oppositely charged to the polyelectrolyte is also found (3).

Adsorption as a function of ionic strength

The influence of the salt concentration upon the adsorption of PSS onto POM crystals was already shown in the previous figures. More detailed results are presented in fig. 8, in which the experimental points (at a constant polyelectrolyte concentration of 67 ppm) were determined in the same way as those of fig. 7. Obviously, a roughly linear relationship exists between adsorbed amount and NaCl concentration, as a result of enhanced screening of segment-segment electrostatic repulsion by the indifferent electrolyte. These results may be compared with literature data. With PSS on preheated silica Marra et al. (8) found the same trend of adsorbed amount increasing

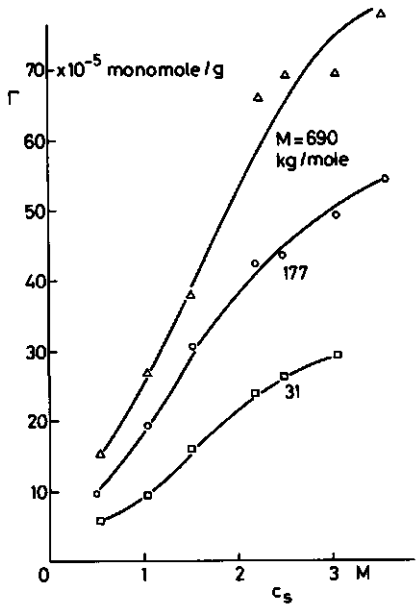

Figure 8: Adsorption of PSS on POM crystals, as a function of NaCl concentration, for three molecular weights. The bulk concentration of PSS was 67 ppm.

linearly with ionic strength. On the other hand, for PSS on platinum (6) and polylysine on AgI (3), the effect of salt concentration c_s is much smaller: for PSS on platinum the adsorption is linear in $\sqrt{c_s}$, for polylysine on AgI the adsorbed amount is proportional to $\sqrt[5]{c_s}$. The weaker dependence of adsorption upon ionic strength for these surfaces can be explained as a consequence of two counteracting effects of the indifferent electrolyte. Screening of the surface and the segmental charges will diminish both the mutual repulsion of charged monomers and the attraction between segments and surface. Adsorption is enhanced by the first effect, whereas the second one works in the opposite direction (although the effect is small if the adsorption energy is high enough). The difference in ionic strength dependence of the adsorption on AgI (3,5) and platinum (6), as compared to POM (fig. 8) and silica (8), may thus be explained by the presence or absence of a surface charge, leading to a high affinity. Hence, these experiments once more indicate the profound effects of an electrostatic contribution to adsorbent-adsorbate affinity in polyelectrolyte adsorption. In the results of Peyser and Ullmann (4) the ionic strength effect cannot be interpreted unambiguously, because the added electrolyte, HCl, will

influence the charge density of the glass surface employed.

Hesselink (2) tabulated theoretical data based on his model for the adsorption of polyelectrolytes, at two different ionic strengths. For an uncharged surface the adsorbed amount was found to increase strongly with the salt concentration, whereas the dependence became much weaker if the surface carried an opposite charge. These results are corroborated qualitatively by Van der Schee's model (3,8). On an uncharged, low-energy surface a linear relationship between adsorption and ionic strength was established (8). A much weaker dependence is predicted for a high-energetic, oppositely charged surface (3). In a general sense, the results with both models agree with our experiments and with the literature data discussed above.

Conclusions

Substantial adsorption of PSS on POM single crystals occurs only at high salt concentrations. The adsorption is characterized by low-affinity isotherms and an approximately linear dependence on log M and on NaCl concentration. These features are characteristic for adsorption on uncharged, low energy surfaces and were also reported by Marra et al. (8) for PSS on preheated silica. With high energy surfaces that have a charge which is opposite in sign to that of the adsorbate, such as hematite, silicate glass, AgI, platinum and $CaCO_3$, always high affinity isotherms are found. Moreover, for the latter surfaces the dependence of adsorption upon molecular weight and salt concentration is much weaker than in case of an uncharged low-energy surface.

The different behaviour on the two types of surfaces can be explained qualitatively in terms of the difference in adsorbent-adsorbate affinity (including electrostatic terms). With a high-energy, oppositely charged adsorbent, most segments lie flat on the surface. The strong interaction between surface and polyelectrolyte segments dominates the adsorption free energy and variations in the polyelectrolyte concentration, molecular weight and ionic strength are only of secondary importance. In the other case, when the attraction of the surface for the polyelectrolyte segments is weak, many segments will

be present in loops and tails. Entropic terms then dominate the adsorption free energy, and a much stronger dependence of the adsorption upon the experimental variables mentioned above is expected.

Acknowledgement

Thanks are due to Mr. J.H. Klunder for carrying out the major part of the adsorption experiments.

References

1. Fleer, G.J., and Lyklema, J., in "Adsorption from solution at the solid/liquid interface," (G.D. Parfitt and C.H. Rochester, Eds.), p. 153. Academic Press, London, 1983.
2. Hesselink, F.Th., J. Colloid Interface Sci. 60, 448 (1977).
3. Van der Schee, H.A., Thesis Agricultural University Wageningen, 1984.
4. Peyser, P., and Ullmann, R., J. Polym. Sci. (A) 3, 3165 (1965).
5. Van der Schee, H.A., and Lyklema, J., in "The effect of polymers on dispersion properties," (Th.F. Tadros, Ed.), p. 81. Academic Press, London, 1983.
6. Takahashi, A., Kawaguchi, M., Hayashi, K., and Kato, T., ACS Symposium Series, 240, 39 (1984).
7. Adam, U.S., and Robb, I.D., J. Chem. Soc., Faraday Trans. 1 79, 2745 (1983).
8. Marra, J., Van der Schee, H.A., Fleer, G.J., and Lyklema, J., in "Adsorption from solution," (R.H. Ottewill, C.H. Rochester and A.L. Smith, Eds.), p. 245. Academic Press, London, 1983.
9. Cohen Stuart, M.A., Scheutjens, J.M.H.M., and Fleer, G.J., J. Polym. Sci. Polym. Phys. Ed. 18, 559 (1980).
10. Papenhuijzen, J., and Fleer, G.J., J. Colloid Interface Sci., to be published.
11. Papenhuijzen, J., Thesis Agricultural University, Wageningen, in preparation.

12. Breeuwsma, A., and Lyklema, J., Discuss. Faraday Soc. 52, 324 (1971).
13. Boyd, G.E., J. Chem. Eng. Data 22, 413 (1977).
14. Cuypers, P.A., Hermens, W.Th., and Hemker, H.C., Anal. Biochem. 84, 56 (1978).
15. Uzgiris, E.E., and Fromageot, H.P.M., Biopolymers 15, 257 (1976).

CHAPTER 5

Polyelectrolyte Adsorption
I. a New Lattice Theory

Introduction

Upon adsorption from solution, the conformation of chain molecules changes drastically. This conformational transition contributes significantly to the free energy and should be taken into account explicitly in any adsorption theory. For adsorption of uncharged polymers, several models have been proposed in the literature. A comprehensive review is given by Fleer and Lyklema (1). Adsorption of flexible polyelectrolytes has much in common with adsorption of uncharged polymers. However, there also exist distinct differences. The most prominent one is the occurrence of long range electrostatic interactions whereas for uncharged polymers only nearest-neighbour interactions play a role.

From any of the models for uncharged polymer a theory for polyelectrolyte adsorption may be developed by incorporating the electrostatic free energy ΔF_e in the partition function of the system. The usual procedure is to consider the total energy of the system as the sum of a non-electrostatic term (which is assumed to be unaffected by the presence of charges) and ΔF_e. About ten years ago, Hesselink (2,3) developed the first primitive model by extending Hoeve's theory (4) for the adsorption of uncharged polymers. Very recently, Van der Schee and Lyklema (5,6) presented a more elaborate model, based on the lattice theory of Roe (7). We start with a short summary of Hesselink's theory, after which a discussion is given of the new lattice theory.

Some of the predictions of these theories have been published. For example, theoretical isotherms have always a high affinity character. The molecular weight dependence is weak at low ionic strength on a high-energy surface carrying a charge of opposite sign to that of the polyelectrolyte. On the other hand, on uncharged, low-energy surfaces

at high ionic strength the adsorbed amount increases rather strongly with molecular weight. The same trend is found with respect to the ionic strength dependence: on low-energy surfaces the effect of indifferent electrolyte concentration is much stronger than on high-energy surfaces. However, a systematic study of the effects of ionic strength, surface charge, chain length, non-electrostatic surface-segment and segment-solvent interactions has, so far, not been reported.

In this paper we present systematic calculations based on the new lattice theory. To this end, the model was extended to account for a charge-free Stern layer adjacent to the surface. We find that the adsorption behaviour is determined first of all by the ionic strength. The non-electrostatic surface-polyelectrolyte interaction is a second important variable, whereas the non-electrostatic segment-solvent interaction and the chain length only play a role at high salt concentration. The polyelectrolyte concentration has hardly any influence at all. On charged adsorbents, we have the intrinsic surface charge as an additional parameter. When the surface and the polyelectrolyte are oppositely charged and when the adsorption is well below monolayer coverage, each additional elementary charge on the surface results in additional adsorption of one segment (for a polyelectrolyte with univalent charge-groups). Apparently, under these conditions, the effects due to the mechanism of charge compensation and to the other adsorptive forces are additional.

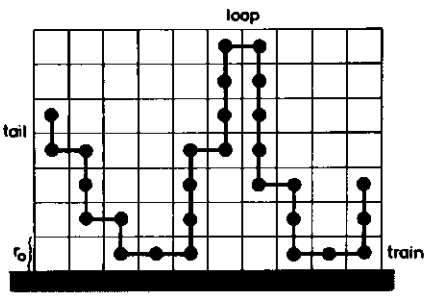

Figure 1: Conformation of an adsorbed polymer chain on a cubic lattice.

Models for polyelectrolyte adsorption

Generally, an adsorbed chain can be considered as a sequence of alternating trains (in which all segments are in direct contact with the surface) and loops consisting of non-adsorbed segments. The segments at either end of the molecule may form free dangling tails. In fig. 1, a conformation of an adsorbed chain in a lattice model is given schematically. In a system with mutually interacting polymer chains, neglect of end effects (tails) greatly simplifies the statistical treatment of polymer adsorption. For this case, only the theory of Scheutjens and Fleer (8) accounts fully for conformations in which tails occur. Unfortunately, the numerical complications arising with this model are considerable, especially if electrostatic terms are included. Tails are neglected in the polymer adsorption theories that are used in the present paper as parent models in the analysis of polyelectrolyte adsoption. In these models the adsorbed layer is assumed to consist of loops and trains only.

Characteristic parameters of the adsorption layer, e.g., adsorbed amount and layer thickness, follow from the partition function Q. In general, Q contains a permutation factor accounting for the possible chain conformations (conformational entropy) as well as energy contributions. Electrostatic effects are incorporated by adding the electrostatic free energy ΔF_e (with respect to a suitable reference state) to the non-electrostatic term ΔF_{ne} which follows from the parent model for uncharged polymer:

$$\Delta F_t = \Delta F_{ne} + \Delta F_e \qquad [1]$$

ΔF_e is obtained from the electrical potential $\psi(x)$ in the system (x being the distance to the surface) by means of a charging process (9). Hence, the first step in any analysis should be the evaluation of such a potential function.

Hesselink's model

Hesselink incorporates electrostatic interactions in Hoeve's model for adsorption of uncharged, flexible polymers. Hoeve's analysis (4) can be summarized as follows. The starting point is the partition function q of an isolated chain at an interface, which contains the adsorption energy and is a function of the average bound fraction p. The excluded volume of loop segments is neglected. For a system of n chains, of which n_σ are adsorbed and n_* are free in solution the canonical partition function Q can be written as:

$$Q = \sum_{n_\sigma, n_*} \Omega(n_\sigma, p) \exp[-\Delta F_m(n_\sigma, p)/kT] \qquad [2]$$

where the factor $\Omega(n_\sigma, p)$ accounts for the number of ways in which n_σ adsorbed molecules (each with partition function q) and n_* molecules in solution can be arranged. Ω contains q and is, therefore, a function of p. It is not a purely entropical factor because of the adsorption energy terms in q. The exponent in the Boltzmann factor represents the free energy of mixing of segments and solvent molecules, but not the adsorption energy. Using the Flory-Huggins theory (10), Hoeve evaluates ΔF_m by assuming an exponential segment concentration profile in the loop layer. The summation in eq. [2] extends over all possible combinations of n_σ and n_*, under the constraint that $n_\sigma + n_*$ is constant.

Hesselink (2,3) introduces the electrostatic contribution ΔF_e to the adsorption free energy in Hoeve's partition function. ΔF_e is evaluated from the potential function $\psi(x)$. For the purpose of calculating $\psi(x)$ Hesselink assumes a step function for the volume fraction ϕ of segments as a function of x:

$$\begin{aligned} \phi &= \phi_t = prn_\sigma v_o/Ar_o && 0 \leq x \leq r_o \\ \phi &= \phi_l = (1-p)rn_\sigma v_o/At && r_o < x \leq t+r_o \\ \phi &= 0 && x > t+r_o \end{aligned} \qquad [3]$$

where r is the number of segments in the polyelectrolyte chain, v_o the segmental volume, t the thickness of the loop layer, r_o the thickness of the layer of adsorbed trains, ϕ_t the volume fraction of segments in the train layer and A the surface area. The average segment volume fraction in the loop layer, ϕ_l, is assumed to be identical to that in a

polyelectrolyte coil in solution according to the Hermans-Overbeek model (11). Usually, this volume fraction is very low and, consequently, irrealistically high values may be found for the layer thickness t at a given amount adsorbed. The use of a step function for the loop layer implies a uniform loop size and constitutes a serious limitation on Hoeve's statistical treatment. Hesselink now proceeds by situating the surface at $x = r_o$, and combines the train charges with the intrinsic surface charge into one overall charge density σ_s. The bulk solution is assumed to be dilute in polyelectrolyte and the segment-free solution between the coils is taken as the reference phase for the potential. If the potentials remain below 50 mV, the Debye-Hückel (DH) approximation may be applied to find the expression for $\psi(x)$ (2,3):

$$\begin{aligned}\psi(x) &= \psi_o \exp\{-\kappa(x-r_o)\} + \\ &\quad - \frac{\tau\alpha e\phi_1}{\varepsilon\kappa^2 v_o}\left[\exp(-\kappa t)\sinh\{\kappa(x-r_o)\} + \right. \\ &\qquad \left. + \exp\{-\kappa(x-r_o)\} - 1\right] \qquad r_o < x \leq t+r_o \\ \psi(x) &= \psi(t+r_o)\exp\{-\kappa(x-t-r_o)\} \qquad x > t+r_o\end{aligned} \qquad [4]$$

In this equation ψ_o is the potential at $x = r_o$, τ the valency of a polyelectrolyte segment (including the sign), α the degree of dissociation of the segments, e the proton charge and ε the dielectric permittivity, considered to be constant throughout the system. The reciprocal thickness of the electical double-layer, κ, is given by:

$$\kappa^2 = 2n_{\pm}e^2/\varepsilon kT \qquad [5]$$

with $n_{\pm}$ the number concentration of positive or negative small ions in the bulk solution, in between the polyelectrolyte coils. ΔF_e is calculated from $\psi(x)$ via a charging process (9); procedure and outcome are given by Hesselink (2,3).

The resulting expression for ΔF_e is now substituted into the partition function Q (eq. [2]), replacing ΔF_m by $\Delta F_m + \Delta F_e$. Hesselink's expression for ΔF_m is slightly modified as compared to the one given by Hoeve, due to the assumption of a step function for the segment concentration profile (eq. [3]). Taking into account that $n_o + n_* =$ constant, Q is simultaneously maximized with respect to n_o and p ($\delta \ln Q/\delta n_o = 0$ and $\delta \ln Q/\delta p = 0$). This results in the equation for the adsorption isotherm:

$$\theta = \phi_t + t\phi_1/r_0 = \phi_* \exp[r\{\eta + \ln(1-p\theta) + 2\chi p\theta - \frac{\tau\alpha\kappa\sigma_s}{2n_\pm e}\}] \qquad [6]$$

which is implicit in θ, the number of segments adsorbed per surface site. In this equation, ϕ_* represents the volume fraction of polyelectrolyte in the bulk solution. In the exponent, the first three terms arise from non-electrostatic contributions in the model. The parameter η is a measure for the non-electrostatic affinity between surface and adsorbate (see also eq. [9], below) and χ is the Flory-Huggins interaction parameter (10). The last term expresses the electrostatic effects, σ_s being the overall charge density in the first layer due to the combined effect of intrinsic surface charge (σ_0) and trains ($\tau\alpha ep\theta$).

Results obtained from Hesselink's adsorption equation (eq. [6]) for negatively charged, univalent, strong polyelectrolyte ($\tau = -1$, $\alpha = 1$) have been presented by the author (3). Adsorption isotherms for long chains are always of the high-affinity type. Tabulated results for an uncharged surface indicate a linear dependence of adsorption on $\sqrt{r}$. This is a typical feature of Hoeve's parent model, preserved despite the simplification introduced by Hesselink. The slope of a plot of θ against $\sqrt{r}$ decreases with increasing non-electrostatic affinity of the surface for the adsorbate. However, no results were given for the molecular weight dependence on a positive surface. The effect of variations in the ionic strength is weaker in the case of strong adsorbent-adsorbate affinity, both for non-electrostatic interactions, represented by η, and for electrostatic interactions due to the presence of a positive intrinsic surface charge.

For the thickness t of the adsorbed layer Hesselink obtains unrealistically large values, of the order of 10 μm. This is a consequence of the simplification introduced with eq. [3].

A new lattice model

Our approach is based on Roe's lattice model for adsorption of uncharged polymer (7). If z is the coordination number of the lattice, each site has $\lambda_0 z$ neighbours in the same layer and $\lambda_1 z$ in each of the

adjacent layers ($\lambda_0 + 2\lambda_1 = 1$). The layers are numbered i = 1,2,...,m where i = 1 is the layer adjacent to the surface. The distance between the lattice layers equals r_o, and a lattice site has an area r_o^2. When adsorption occurs, the segmental concentration is highest in layer 1 whereas in layer m+1, m+2, etc. it equals the bulk concentration. In each layer parallel to the surface we assume random mixing (mean field approximation). The volume fraction of segments in layer i is indicated by ϕ_i. The general expression for the (maximum term of the) partition function Q is:

$$Q = \Omega(\{\phi_i\})\exp[-\Delta F_t(\{\phi_i\})/kT] \qquad [7]$$

where $\Omega(\{\phi_i\})$ is the number of ways in which a segment concentration profile $\{\phi_i\}$ with (free) energy ΔF_t can be obtained. In contrast to Hoeve's model, Ω is a purely combinatorial factor representing the conformational entropy and the entropy of mixing of segments and solvent. ΔF_t contains the adsorption energy, the contact (free) energy of segments and solvent and, for polyelectrolytes, the electrostatic free energy ΔF_e as independent terms. The contribution of each polymer segment to ϕ_i is assumed to be independent of its position along the chain (e.g., in the middle part or near one of the ends). This assumption is equivalent to the neglect of tails (1,8). Contrary to Hoeve (4), Roe (7) considers an open system with the chemical potentials in the bulk solution constant. The partition function Q is maximized with respect to ϕ_i to give the equilibrium segment concentration profile $\{\phi_i\}$. For the case that $\Delta F_e = 0$, the resulting equation was given by Roe (eq. [29] of ref. (7)). Adding a term $\delta\Delta F_e/\delta\phi_i$ to the result, we can write:

$$\frac{\delta\Delta F_e(\{\phi_i\})}{kT.\delta\phi_i} + 2\chi(<\phi_i>-\phi_*) + (\chi_s+\lambda_1\chi)\delta_{1,i} + \ln\{\phi_*/(1-\phi_*)\} + \ln\{(1-\phi_i)/\phi_i\} + (1-1/r)[\ln(<\phi_i>/\phi_i) + <\phi_i/<\phi_i>> - 1] = 0 \qquad (i = 1,2,...,m) \qquad [8]$$

In this equation $\delta_{1,i}$ is the Kronecker delta ($\delta_{1,i} = 1$ for i = 1 and 0 for $i \neq 1$) and χ_s a dimensionless adsorption energy parameter, related to Hesselink's adsorption energy parameter η by:

$$n = \chi_s - \chi_{sc} \qquad [9]$$

where χ_{sc} is the critical adsorption energy parameter, defined as $\chi_{sc} = -\ln(1-\lambda_1)$ (7,8). The angular brackets denote averages over the layers i-1, i and i+1. For example, $\langle\phi_i\rangle$ is given by:

$$\langle\phi_i\rangle = \lambda_1\phi_{i-1} + \lambda_0\phi_i + \lambda_1\phi_{i+1} \qquad [10]$$

and $\langle\phi_i/\langle\phi_i\rangle\rangle$ is a similar average of $\phi_i/\langle\phi_i\rangle$. For uncharged polymers the electrostatic term vanishes and the segment profile $\{\phi_i\}$ is obtained as the solution of the m simultaneous equations as given in [8].

For polyelectrolyte adsorption, we have to find first the electrostatic term ΔF_e as a function of $\{\phi_i\}$. It is calculated assuming that the segmental charges may be considered to be smeared out in planes parallel to the surface, through the centers of the lattice cells (plane charges). The distribution of the small ions, considered as point charges, is governed by the potential due to the charged planes and the surface charge.

In fig. 2 we give a schematic representation of the potential profile for a negatively charged polyelectrolyte, near a positive surface and in the bulk solution. If the potential distribution in the system is known, ΔF_e follows from a charging process (9). We first evaluate the contribution $\Delta F_e^{(i)}$ due to only the polyelectrolyte charges in layer i. To this end we envisage a charging process, in which charged segments are transferred from the bulk solution to layer i (5):

$$\Delta F_e^{(i)} = r_o^2 \left[\int_{\sigma_*}^{\sigma_i} \psi_i' d\sigma' - \int_{\sigma_*}^{\sigma_i} \psi_* d\sigma' \right] \qquad [11]$$

The first term on the right hand side represents the charging of layer i and the second one stands for the de-charging of a bulk layer. We consider an open system and therefore the potential ψ_*, at the position of plane charge in the bulk solution, remains constant during the process. Eq. [11] represents the charging of plane i, starting from the plane charge density in the bulk, σ_*, to the final value σ_i. σ_* and σ_i are defined as:

$$\sigma_* = \tau\alpha e\phi_*/r_o^2$$
$$\sigma_i = \tau\alpha e\phi_i/r_o^2 \qquad [12]$$

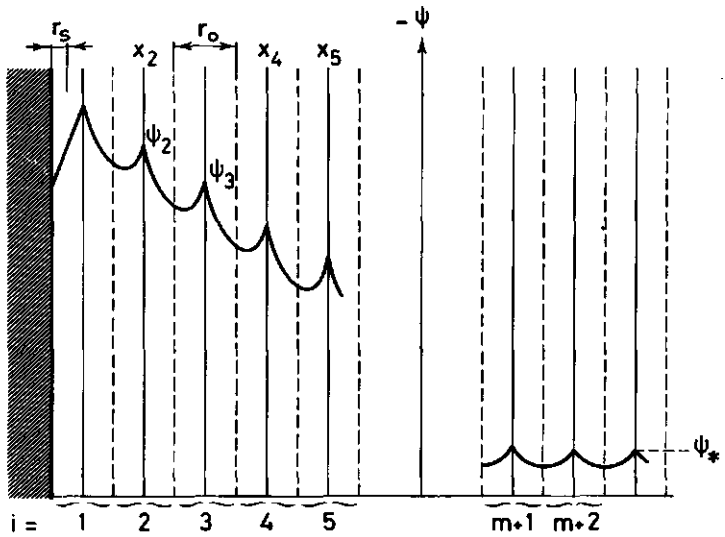

Figure 2: Schematic potential profile for a negatively charged polyelectrolyte near a positive surface (layer i = 1, 2, ..., m), and in the bulk solution (layer i = m+1, m+2, ...). The distance between the lattice layers equals r_o. Adjacent to the surface a Stern layer of thickness $r_s = r_o/4$ is assumed.

At any moment during the charging process, the plane charge density and the potential at the position $x = x_i$ of plane i are given by σ' and ψ_i', respectively. The final values are σ_i and ψ_i. ψ_i corresponds to the peak in fig. 2 at distance $x = x_i$ from the surface, at the centre of layer i. Note that ΔF_e as given in [11] is expressed per surface site, with area r_o^2. The free energy is an additive quantity, and therefore [11] may be generalized for m lattice layers. By combining the integrals we obtain:

$$\Delta F_e = \sum_{i=1}^{m} \int_{\sigma_*}^{\sigma_i} (\psi_i' - \psi_*) d\sigma' \qquad [13]$$

According to eq. [8], we do not need ΔF_e itself, but only the derivative $\delta\Delta F_e/\delta\phi_i$. With [12] we have $\delta\Delta F_e/\delta\phi_i = (\tau\alpha e/r_o^2)\delta\Delta F_e/\delta\sigma_i$. Hence:

$$\delta\Delta F_e/\delta\phi_i = \tau\alpha e(\psi_i - \psi_*) \qquad (i = 1,2,\ldots,m) \qquad [14]$$

which may be inserted into eq. [8]. The only remaining problem is to find the potential profile $\{\psi_i\}$ (the peak values in fig. 2), given the segment concentration profile $\{\phi_i\}$.

We consider the potential in an array of plane charges (fig. 2). First we have to define a suitable reference state. An obvious choice would be a polyelectrolyte-free salt solution separated from the polyelectrolyte system by a membrane. In such a solution the potential is zero by definition. However, the salt concentration in it is related to the composition of the polyelectrolyte solution, through a Donnan equilibrium, and therefore unknown a priori. We choose the reference potential at some position in the bulk polyelectrolyte solution. In a lattice model, this bulk solution consists necessarily also of lattice layers in which the potential and the concentrations of small ions vary periodically (see fig. 2). Adsorption experiments are usually carried out at polyelectrolyte concentrations in the bulk solution that are below 1000 ppm (v/v). This implies low plane charge densities σ_* and, consequently, low potentials. By application of the DH approximation in the lattice model for the bulk solution it can be shown that the positive and the negative small ions (including those originating from the polyelectrolyte) are at their stoichiometric concentrations at a potential $\bar{\psi}$ that is given by (5):

$$\bar{\psi} = \sigma_*/\varepsilon\kappa^2 r_o \qquad [15]$$

$\bar{\psi}$ as calculated from eq. [15] is some average of the periodic potential function in the bulk solution (fig. 2). We take $\bar{\psi}$ as the reference potential. The reciprocal shielding length κ in [15] is defined as a function of stoichiometric concentrations ($\bar{n}_+$, $\bar{n}_-$) of small ions:

$$\kappa^2 = (\bar{n}_+ + \bar{n}_-)e^2/\varepsilon kT \qquad [16]$$

This expression for κ differs from that in eq. [5], as the latter is given in terms of the concentration of the added indifferent electrolyte only, not including the counterions of the polyelectrolyte.

Having defined the reference potential, we can immediately write down the Poisson-Boltzmann (PB) equation for the potential $\psi(x)$ at a distance x from the surface:

$$d^2\psi(x)/dx^2 = \frac{-e}{\varepsilon}\,[\bar{n}_+ \exp\{-e(\psi(x)-\bar{\psi})/kT\} + - \bar{n}_- \exp\{e(\psi(x)-\bar{\psi})/kT\}] \qquad [17]$$

In the case of high potentials (occurring locally at low ionic strength) eq. [17] must be solved for $\psi(x)$ by numerical integration. In many cases, especially for high salt concentrations, the potential remains low throughout the system and an analytical solution of [17] can be obtained using the DH approximation. Linearization of the PB equation [17] and substitution of $\bar{\psi}$ (eq. [15]), with the expression for κ given in [16], yields (5):

$$d^2\psi(x)/dx^2 = \kappa^2\psi(x) \qquad [18]$$

This simple form, in which $\bar{\psi}$, σ_* nor r_0 occur explicitly, is obtained by virtue of the choice for the reference state. If only one charged plane would be present at $x = x_j$, solution of eq. [18] using the appropriate boundary conditions at $x = 0$, $x = x_j$ and $x = \infty$, yields:

$$\psi(x) = \frac{\sigma_j}{2\kappa\varepsilon}\,[\exp(-\kappa|x-x_j|) + \exp\{-\kappa(x+x_j)\}] \qquad [19]$$

The second term on the right hand side of eq. [19] may be regarded to represent the effect of image charges. If the surface charge σ_0 is zero the potential at the planes (at $x = ir_0$) follows by summing the contributions due to all plane charges in the system:

$$\psi_i^p = \sum_{j=1}^{\infty} \frac{\sigma_j}{2\kappa\varepsilon} [\exp(-\kappa r_o|i-j|) + \exp\{-\kappa r_o(i+j-1)\}] \qquad [20]$$

where the superscript p denotes the contribution due to the presence of polyelectrolyte. The potential at the position of a plane charge in the bulk solution follows as a summation of symmetric plane potentials:

$$\psi_* = \frac{\sigma_*}{2\kappa\varepsilon} \sum_{p=-\infty}^{\infty} \exp(-\kappa r_o|p|) = \frac{\sigma_*}{2\kappa\varepsilon} \frac{1 + \exp(-\kappa r_o)}{1 - \exp(-\kappa r_o)} \qquad [21]$$

The model may be extended by introducing a charge-free Stern layer with a thickness r_s. We assume $r_s \leq r_o/2$. Applying the appropriate boundary conditions, we obtain for ψ_i^p:

$$\psi_i^p = \sum_{j=1}^{\infty} \frac{\sigma_j}{2\kappa\varepsilon} [\exp(-\kappa r_o|i-j|) + \exp(2\kappa r_s)\exp\{-\kappa r_o(i+j-1)\}] \qquad [22]$$

Eq. [22] gives the potential due to the polyelectrolyte charges. If the surface is charged, an additional contribution ψ_i^σ should be considered. This contribution follows from eq. [19] by substituting $x_j = 0$, $\sigma_j = \sigma_o$ and taking into account the presence of a Stern layer:

$$\psi_i^\sigma = \frac{\sigma_o}{\kappa\varepsilon} \exp\{-\kappa(x_i - r_s)\} = \frac{\sigma_o}{\kappa\varepsilon} \exp(\kappa r_s)\exp\{-\kappa r_o(i-1/2)\} \qquad [23]$$

The potential ψ_i to be used in [14] is the sum of ψ_i^p and ψ_i^σ as given in [22] and [23]. For the computations, the summation in [22] may be split up in the parts $1<j<m$ and $j>m$. For the second part an analytical solution can be found, representing the contribution of the bulk solution to ψ_i.

In the case of strong adsorption at low ionic strength, the potential in the first layers near the surface may be locally too high for the DH approximation to be valid. For these layers the PB equation is solved by numerical integration from one plane charge to the other. In the outer layers the DH approximation can still be applied.

Eqs. [22] - [23] express ψ_i as a function of all plane charges. By means of [12] $\{\sigma_i\}$, and hence $\{\psi_i\}$, is immediately found as a function of the segment concentration profile $\{\phi_i\}$. Substitution of ψ_i in [14]

and combination with [8] yields a set of m implicit equations from which the segment concentration profile $\{\phi_i\}$ may be solved numerically. The excess surface coverage θ_{ex} now follows as:

$$\theta_{ex} = \sum_{i=1}^{m} (\phi_i - \phi_*) \qquad [24]$$

This quantity becomes equal to θ (eq. [6]) only in case of strong adsorption from dilute solution. Direct evaluation of θ, however, is not possible in the present model since ϕ_i is made up of contributions due to segments of adsorbed as well as unadsorbed chains, which cannot be distinguished. This limitation is inherent to the Roe model. The root-mean-square thickness of the adsorption layer t_{rms}, expressed in numbers of lattice layers, is given by:

$$t_{rms}^2 = \frac{1}{\theta_{ex}} \sum_{i=1}^{m} i^2 (\phi_i - \phi_*) \qquad [25]$$

Results and discussion

Some preliminary results obtained with the lattice theory for polyelectrolyte adsorption have been published before, for a rather limited choice of parameters. One set of results (5,6) applies to adsorption at low ionic strength on a high-energy surface carrying a charge of opposite sign to that of the polyelectrolyte, and in another paper (12) data were given for adsorption at high ionic strength on an uncharged, low-energy surface. In these computations, the effect of the Stern layer was not considered. We present here a selection of predictions obtained by varying systematically the relevant parameters, taking into account the presence of a Stern layer. One purpose is to show the typical differences in adsorption behaviour at high surface-polyelectrolyte affinity, as compared to situations where adsorbent-adsorbate interactions are weak. In the first case adsorption occurs at low ionic strength and is characterized by high-affinity isotherms, flat adsorbed layers and weak dependence upon molecular weight and salt concentration. In the second situation substantial adsorption occurs only at high ionic strength and is distinguished by

thicker adsorbed layers and stronger effects of molecular weight and ionic strength.

The first task is to select the various parameters. With uncharged polymers, five parameters determine the adsorbed amount θ_{ex}, expressed in equivalent monolayers or segments per surface site. These are the lattice parameter λ_0, the number of segments per chain r, the Flory-Huggins parameter χ, the adsorption energy parameter χ_s and the volume fraction ϕ_* of polymer in the bulk solution. θ_{ex} does not depend on r_0. The surface area r_0^2 of the lattice cell is merely needed to convert the theoretical adsorption (segments per surface site) into experimental units (monomole/m^2). In the analysis of polyelectrolyte adsorption, a realistic choice for r_0 is far more important because here the interlayer distance affects directly the potential profile in the adsorption layer, and thus also the theoretical adsorption θ_{ex}. For a larger r_0 lower potentials develop and, consequently, greater values are found for θ_{ex}. Apart from r_0, we have with polyelectrolytes another three parameters that are entirely due to the electrostatics: the Sternlayer thickness r_s, the surface charge density σ_0 and the salt concentration c_s.

We do not treat λ_0, r_0 and r_s as adjustable parameters. For λ_0 we take a value of 0.5, corresponding to a hexagonal lattice. The parameter r_0 is related to the separation between neighbouring charges on the polyelectrolyte. According to the concept of counterion condensation (13), the distance between two effective charges of a highly charged polyelectrolyte equals the Bjerrum length, which is 0.71 nm if the dielectric permittivity ε is taken as that of pure water. However, the dielectric permittivity at the position of a segment is determined not only by the medium, but also by the two neighbouring segments on the chain, which have a much lower value of ε. This results in a lower average value for ε (14) and, consequently, a larger Bjerrum length is found. In the calculations presented here we adopt a value of 1 nm for r_0. In this way, r_0 does not depend on the chemical nature of the polyelectrolyte concerned.

The Stern layer thickness r_s mainly affects the potential in the vicinity of the surface, and adjustment of this parameter may be effectively counterbalanced by variations in the adsorption energy χ_s. For r_s we take a value corresponding approximately to the radius of a

hydrated counterion: r_s = 0.25 nm.

We studied the effects of the remaining five parameters on polyelectrolyte adsorption by considering the dependence of θ_{ex} upon ϕ_*, c_s and r. These are the relevant relationships from an experimental point of view, because the adsorbed amount can easily be determined as a function of polyelectrolyte concentration, ionic strength and molecular weight. For the other three parameters (σ_o, χ_s and χ) we choose two values, each of which corresponds more or less to reasonable extremes in experimental situations. The surface charge density σ_o is either taken to be zero (uncharged surface) or 0.25 elementary charges per lattice site (σ_o = + 0.04 C/m^2, typical of a highly charged surface). For the non-electrostatic adsorption energy we use χ_s = 0.5 (not too far above the critical value 0.288) and χ_s = 4 (strong adsorption). For the segment-solvent interaction it is difficult to make a choice which is supported by experimental evidence. Measurement of the second virial coefficient in polyelectrolyte solutions gives always an effective interaction parameter, in which the electrostatic interaction is included. Most polyelectrolytes would not be soluble in water if the charges were absent, and therefore χ is probably high. We take as representative values χ = 0.5 (a relatively good solvent for a polyelectrolyte) and χ = 1. The latter value corresponds to a polyelectrolyte for which phase separation occurs at a salt concentration around 4 M, such as polystyrene sulfonate in NaCl-solutions (15,16). Calculations were carried out for a negatively charged, strong polyelectrolyte (τ = -1, α = 1) in the presence of univalent indifferent electrolyte. In most cases the DH approximation could be applied. However, for strong adsorption (χ_s = 4) at low salt concentration ($c_s \leq 0.1$ M) high potentials develop and the PB equation was solved by numerical integration. Hence, all results may be considered as having been obtained with the full PB-equation.

Typical segment concentration profiles are given in fig. 3, with a logarithmic scale for ϕ_i. We compare an uncharged polymer with a strongly charged polyelectrolyte. The data in fig. 3a represent adsorption at low c_s on a high-energy, charge bearing surface, whereas fig. 3b applies to high c_s and a low-energy, uncharged surface. The minimum in the profiles is a consequence of repulsion between unadsorbed chains and the covered surface, of which the overall charge has the same

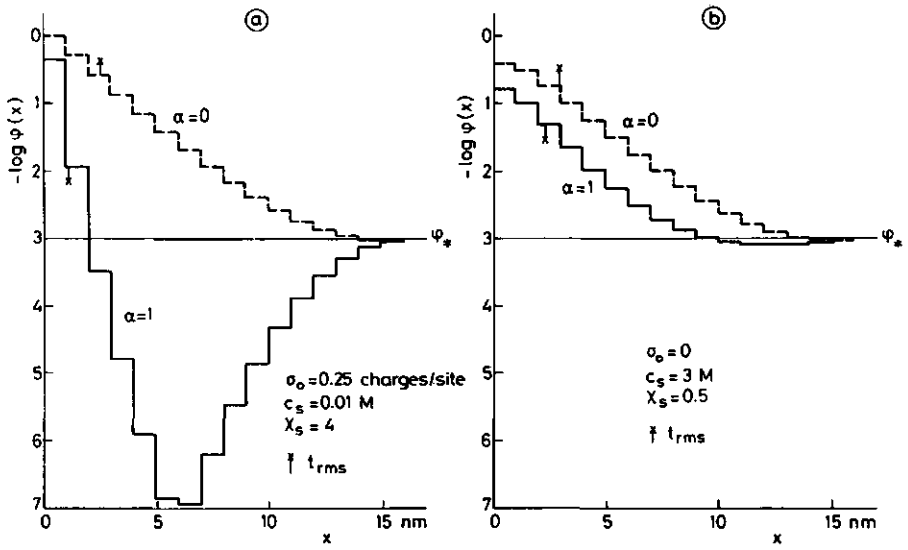

Figure 3: Segment concentration profiles in the adsorption layer, for negatively charged, strong polyelectrolyte ($\tau = -1$, $\alpha = 1$), on an uncharged surface (a) and on a positively charged surface (b). The root-mean-square thickness of the adsorption layer t_{rms} is indicated in the figures. $r = 500$, $\chi = 0.5$.

sign as the polyelectrolyte. It is more pronounced when χ_s is high and c_s low. Note, however, that the minimum is only obvious with a logarithmic scale for ϕ_i: even in fig. 3a it would hardly have been noticed with a linear scale for ϕ_i.

For each segment profile the corresponding root-mean-square layer thickness t_{rms} is indicated in the figure. The values found are of the order of 2 nm, which is far more realistic than the enormous thicknesses obtained with Hesselink's model. Clearly, the fact that in our model no a priori assumptions are required as to the segment concentration profile constitutes a major improvement over Hesselink's theory. We observe in fig. 3a that t_{rms} is much smaller for the polyelectrolyte than for the uncharged polymer. This points to a very flat conformation at low salt concentrations. At high c_s, t_{rms} for the polyelectrolyte is only slightly below the value for the uncharged polymer (fig. 3b), indicating a similar conformation of the adsorbed chains with more and

longer loops. Yet, the segment profile differs significantly from that of uncharged polymer. Apparently, complete screening of the segment-segment repulsion does not occur, not even at salt concentrations as high as 3 M.

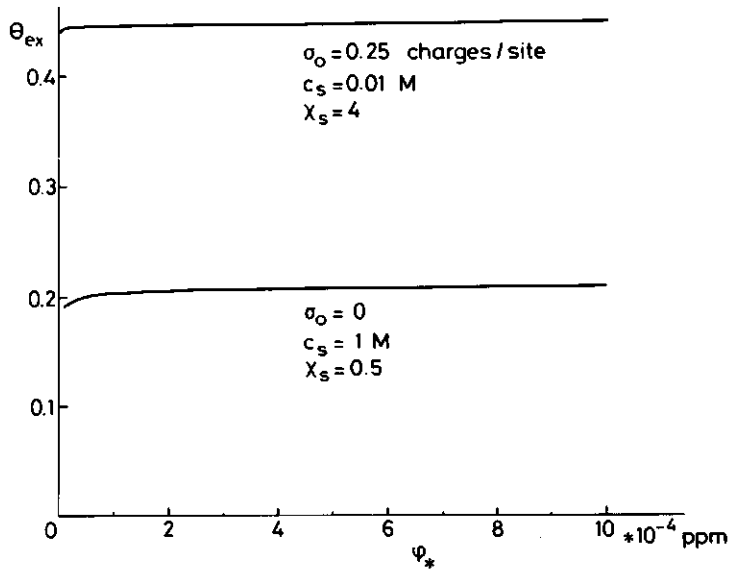

Figure 4: Adsorption isotherms on low- and high-affinity surfaces. $\tau = -1$, $\alpha = 1$, $r = 500$ and $\chi = 0.5$.

In fig. 4 we give adsorption isotherms that apply to two widely different situations: adsorption at low ionic strength on a high-energy, strongly charged surface, as compared to adsorption at high c_s on a low-energy, uncharged surface. Although the adsorbed amounts differ significantly, the shape of the isotherms is nearly the same. Both isotherms exhibit a high-affinity character. Effects of the various parameters show up only in the plateau value of the isotherms. In the next figures, we discuss the dependence of the adsorbed amount on the salt concentration and the chain length, at $\phi_* = 0.00004$ and at $\phi_* = 0.001$. Results for different values of ϕ_* are essentially the same, as can be seen clearly in fig. 4.

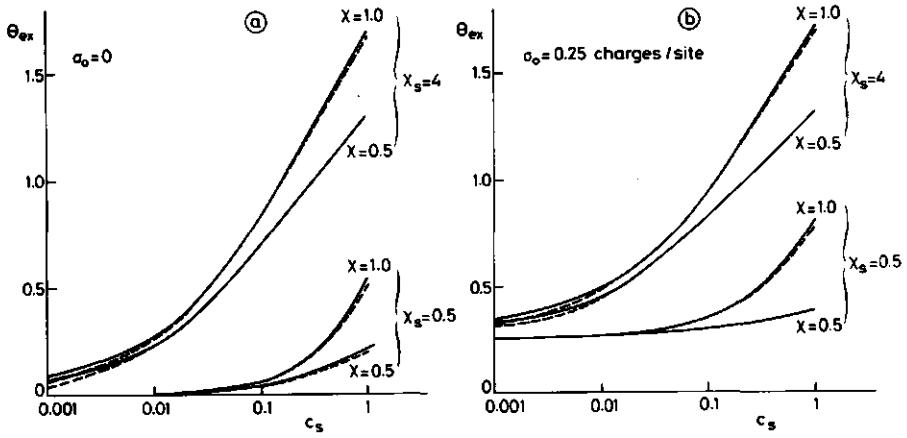

Figure 5: Adsorption as a function of ionic strength on an uncharged surface (a) and on a positively charged surface (b). The bulk solution concentration ϕ_* is 40 ppm (dashed curves) or 1000 ppm (full curves). $\tau = -1$, $\alpha = 1$ and $r = 500$.

Plots of θ_{ex} vs. log c_s are given in fig. 5. In the curves two regimes can be distinguished. For $c_s \leq 0.01$ M the dependence of θ_{ex} upon log c_s is weak and the effects of variations in χ are small. On an uncharged surface (fig. 5a) at low χ_s hardly any adsorption is found under these conditions. Adsorption at low c_s occurs only if either strong electrostatic interaction (large, positive σ_o) or a strong non-electrostatic affinity (high χ_s) is present. In this region of low adsorption, an increase of the surface charge from zero to 0.25 elementary charges per surface site gives rise to an additional adsorption of 0.25 polyelectrolyte segments per site. Hence, each additional elementary charge on the surface leads to an extra adsorption of one segment.

At high ionic strength ($c_s \geq 0.1$ M) a much stronger dependence of θ_{ex} upon log c_s is found. Also the effects of variations in χ are more pronounced, whereas those of χ_s remain invariably strong. At high χ_s and high c_s the effect of the surface charge is weak; in this case the non-electrostatic part of the affinity dominates the adsorption process.

The trends observed in fig. 5 are interpreted as follows. At low c_s, the segment-segment repulsion almost completely offsets the driving force for adsorption arising from non-electrostatic segment-surface interactions. Then the adsorption is weak and nearly invariant with χ and c_s, whereas the two contributions to the adsorbent-adsorbate affinity, determined by σ_o and χ_s, influence the adsorbed amount independently. Screening of the segment-segment repulsion at high ionic strength presents the main cause for the stronger dependence of the adsorption upon c_s and χ, both for uncharged and for positively charged surfaces. Apparently, at high c_s interactions of the polyelectrolyte with the solvent become a more important factor in the adsorption process, just as for uncharged polymers. When also χ_s is high, the surface charge is seen to have only a weak effect on the adsorption, which is well above monolayer coverage. In this situation, it could be envisaged that the adsorption is restricted by the excluded volume of the already adsorbed segments rather than by electrostatic segment-segment repulsion. The effective non-electrostatic excluded volume is related to the segment-solvent interaction parameter χ. Our interpretation is, therefore, in line with the observation in fig. 5 that under these conditions the adsorption is strongly affected by the value of χ.

In fig. 6 we give the adsorption θ_{ex} as a function of log r, at low ionic strength (0.01 M), again for an uncharged (fig. 6a) and for a positively charged surface (fig. 6b). Note that the ordinate scale has been expanded by a factor three as compared to fig. 5. As before, the polyelectrolyte concentration hardly affects the results. At low c_s, the effect of segment-solvent interactions (χ) is of minor importance and an increase of the surface charge results in an equivalent additional adsorption (see also fig. 5). The adsorbed amount at this low ionic strength does not depend on the chain length for any value of χ, χ_s and σ_o. This can be explained as a consequence of strong segment-segment repulsion, which overrules completely the effects due to changes in the conformational entropy. It also correlates with the observation made in the discussion of fig. 3a, that at low ionic strength the adsorbed chains lay essentially flat on the surface.

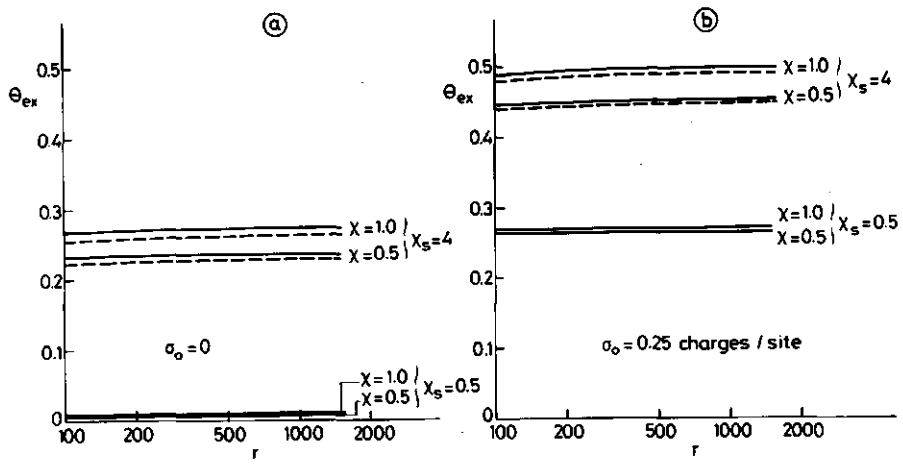

Figure 6: Adsorption as a function of chain length at c_s = 0.01 M, on an uncharged surface (a) and on a positively charged surface (b). The bulk solution concentration ϕ_* is 40 ppm (dashed curves) or 1000 ppm (full curves). τ = -1 and α = 1.

The dependence of θ_{ex} upon log r at high c_s (1 M) is illustrated in fig. 7, with the ordinate scale the same as in fig. 5. In line with fig. 5, at c_s = 1 M the effect of χ upon the adsorbed amount is stronger as compared to the situation at c_s = 0.01 M (see also fig. 6).
Once more, at high c_s equivalent adsorption in relation to the surface charge is found to occur only at low χ_s. Contrary to the situation at low c_s, a significant increase is now found for θ_{ex} as a function of log r. This confirms results of Marra et al. (12) and may be ascribed to enhanced screening of the segmental charges, as a consequence of which conformational entropy terms become relatively more important in the adsorption free energy. In this respect, adsorption of polyelectrolytes at high salt concentrations resembles to some extent that of uncharged polymer, although quantitative differences remain (see also the discussion of fig. 3b). In the Roe-theory, the parent model for our polyelectrolyte adsorption theory, end effects (tails) are neglected. For uncharged polymers, Scheutjens and Fleer (8) showed that this results in a weaker dependence of adsorption upon r as compared to

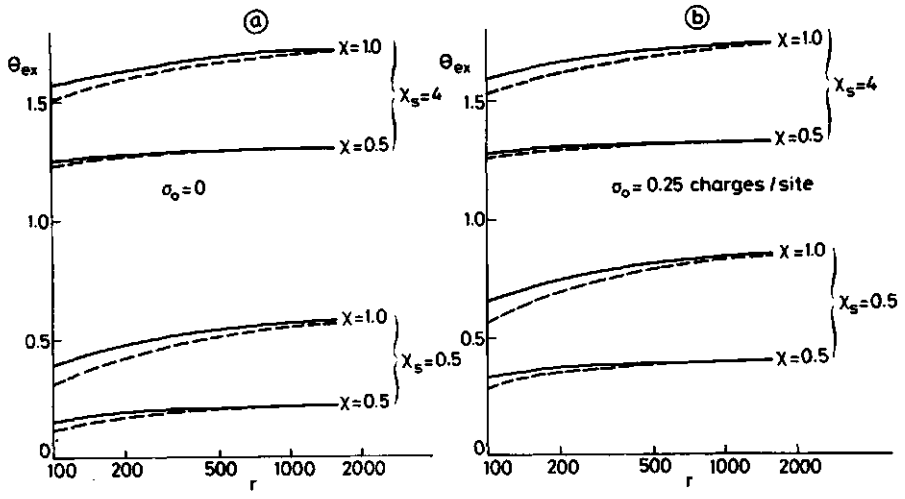

Figure 7: Adsorption as a function of chain length at c_s = 1 M, on an uncharged surface (a) and on a positively charged surface (b). The bulk solution concentration ϕ_* is 40 ppm (dashed curves) or 1000 ppm (full curves). τ = -1 and α = 1.

their model in which tails are properly taken into account. Consequently, we expect that our present model underestimates the dependence of θ_{ex} upon chain length at high ionic strength, especially for long chains.

Conclusions

By incorporating an electrostatic contribution into the Roe theory for the adsorption of uncharged polymers, a new lattice theory for polyelectrolyte adsorption could be formulated. The model is much more sophisticated than a previous one of Hesselink, because no a priori assumption for the segment concentration profile is required and the excluded volume of loop segments is taken into account. Yet it has at least two disadvantages. The first is that the Roe model neglects tails, which may be important at high salt concentrations. This could be improved only by replacing the Roe model by the Scheutjens-Fleer

model. The latter accounts properly for the occurrence of tails. Some preliminary results have been obtained with such an analysis, but so far numerical complications prevented systematic calculations. The second problem is the use of a mean field approximation. This may be justified in the adsorbed layer, where the segment concentration is relatively high, but is dubious for the bulk of the solution where the individual coils do not overlap. Therefore, the dependence of the various adsorbed layer characteristics on the bulk solution concentration could be less reliable in the present model.

Qualitatively, both Hesselink's model and ours predict the same trends: a relatively strong increase of adsorption with r and c_s for low-energy, uncharged surfaces at high ionic strength and a much weaker dependence of the adsorbed amount upon r in case of a high-energy surface carrying a charge of opposite sign to that of the polyelectrolyte.

Systematic calculations with the new lattice model show that the ionic strength determines how the adsorbed amount varies with the salt concentration and the chain length. In both cases the strongest dependence is found at high c_s. Non-electrostatic segment-solvent interactions (χ) are also more important under these conditions. The non-electrostatic surface-polyelectrolyte affinity (χ_s) always has a pronounced influence. In the presence of a surface charge of opposite sign to that of the polyelectrolyte, each elementary charge on the surface corresponds with the adsorption of one segment. Only for a high-affinity surface at high c_s is this charge compensation not found, because in this situation the hard core excluded volume of the segment rather than the electrostatic repulsion limits the adsorption. For the thickness of the adsorbed layer we obtained 2 to 5 nm with the new lattice model, which is more realistic than previous results of Hesselink.

References

1. Fleer, G.J., and Lyklema, J., in "Adsorption from Solution at the Solid/Liquid Interface" (G.D. Parfitt and C.H. Rochester, Eds.), p. 153. Academic Press, London, 1983.

2. Hesselink, F.Th., J. Electroanal. Chem. 37, 317 (1972).
3. Hesselink, F.Th., J. Colloid Interface Sci. 60, 448 (1977).
4. Hoeve, C.A.J., J. Polym. Sci. (C) 34, 1 (1971).
5. Van der Schee, H.A., Thesis Agricultural University, Wageningen, 1984.
6. Van der Schee, H.A., and Lyklema, J., J. Phys. Chem., submitted.
7. Roe, R.-J., J. Chem. Phys. 60, 4192 (1974).
8. Scheutjens, J.M.H.M., and Fleer, G.J., J. Phys. Chem. 83, 1619 (1979) and 84, 178 (1980).
9. Verwey, E.J.W., and Overbeek, J.Th.G., "Theory of the Stability of Lyophobic Colloids," p. 62. Elsevier Publishing Company, Inc., Amsterdam, 1948.
10. Flory, P.J., "Principles of Polymer Chemistry," p. 508. Cornell University Press, Ithaca, 1953.
11. Hermans, J.J., and Overbeek, J.Th.G., Rec. Trav. Chim. 67, 761 (1948).
12. Marra, J., Van der Schee, H.A., Fleer, G.J., and Lyklema, J., in "Adsorption from Solution," (R.H. Ottewill, C.H. Rochester and A.L. Smith, Eds.), p. 245. Academic Press, London, 1983.
13. Manning, G.S., J. Chem. Phys. 51, 924 (1969).
14. Böttcher, C.J.F., "Theory of Electric Polarization," p. . Elseviers Publishing Company, Inc., Amsterdam, 1952.
15. Papenhuijzen, J., Fleer, G.J., and Bijsterbosch, B.H., J. Colloid Interface Sci., part II of this paper.
16. Takahashi, A., Kato, T., and Nagasawa, M., J. Phys. Chem. 71, 2001 (1967).

CHAPTER 6

Polyelectrolyte Adsorption
II. Comparison of Experimental Results for Polystyrene Sulfonate, Adsorbed on Polyoxymethylene Crystals, with Theoretical Predictions

---

Introduction

In the preceding paper (1) we discussed two models for adsorption of flexible polyelectrolytes, one due to Hesselink (2,3) and the other to Van der Schee and Lyklema (4,5). Here we will only consider the latter one which is more elaborate and incorporates some fundamental improvements as compared to Hesselink's approach. It is based on Roe's lattice theory for adsorption of uncharged polymer (6). The electrostatic contribution is evaluated by assuming the polyelectrolyte charges to be smeared out in planes parallel to the surface. From the potential at the position of the planes the electrostatic contribution to the overall free energy of adsorption is calculated. Minimization of the overall adsorption free energy yields the segment concentration profile in the layers near the surface. From this the excess adsorbed amount follows readily.

The theory has been compared with experimental data by Van der Schee and Lyklema (5), who adsorbed polylysine (at pH 1, where it is positively charged) on negative AgI, and by Marra et al. (7) using homodisperse polystyrene sulfonate (PSS) on preheated silica. With polylysine on AgI adsorption occurs already at low salt concentration and the effects of polyelectrolyte concentration, ionic strength and molecular weight are weak. For the adsorption of PSS on silica a high salt concentration is required and the dependence upon polyelectrolyte concentration, ionic strength and molecular weight is much stronger. Qualitatively, the experimental dependences on salt concentration and molecular weight were confirmed by the theoretical calculations (5,7). However, the shape of the theoretical (sharp)

isotherms did only agree with results for polylysine on AgI (5). For PSS on silica rounded isotherms were found (7).

As a further test of the theory, we carried out adsorption measurements with polyoxymethylene (POM) crystals as the adsorbent. These can be obtained in the form of hexagonal platelets of uniform thickness, and have a chemically homogeneous surface (consisting entirely of ether groups) that carries virtually no charge. This is important, because the presence of a surface charge might give rise to complications: adsorbed polyelectrolyte affects the activity of potential determining ions near the surface (Donnan effect) and probably also their specific adsorption behaviour. From the adsorption plateau of a non-ionic surfactant a value of 60 m^2/g was derived for the specific surface area of POM crystals suspended in water. The methods of preparation and characterization of the crystals are given more extensively elsewhere (8).

As the adsorbate we used PSS, a strong polyelectrolyte that can be purchased in the form of homodisperse samples. With such a strong polyelectrolyte the charge density along the chain does not depend upon the local segment concentration. Also, we do not have to account for heterodispersity as a possible cause for roundedness of the measured isotherms (9). Ten samples were obtained, which we characterized with various techniques. The results have been reported before (10): five of the ten samples (ex Pressure Chemical Co.) are not sufficiently reliable on account of the characteristics (elemental analysis, extinction coefficient, viscosity) examined. The remaining five samples are those of M = 31, 88, 177, 354 and 690 kg/mole.

The adsorption of PSS on POM crystals was measured as a function of chain length, expressed in the number of segments r, salt concentration c_s and polyelectrolyte concentration in the bulk solution ϕ_* (v/v). The experimental procedure and a qualitative discussion of the results have been presented before (11). Substantial adsorption occurs only at high ionic strength and the measured isotherms are rounded. The adsorbed amount increases approximately linearly with c_s and log r. These features were also reported by Marra et al. (7) for PSS on silica, and contrast sharply with the data of Van der Schee and Lyklema (5) for polylysine on AgI. We explained the results in terms of differences in the adsorbent-adsorbate affinity (11). Strong interaction is expected

between polylysine and (oppositely charged) AgI, whereas much weaker attraction will occur between PSS and silica (carrying a small charge of the same sign as PSS) or POM. POM is an uncharged adsorbent of organic nature. Consequently, electrostatic interactions with the polyelectrolyte are absent and non-electrostatic interactions are not expected to be very strong, due to the weak dispersion forces that are generally found for organic materials. In the preceding paper (1) we presented systematic calculations that confirm these trends.

In order to compare qualitatively our experimental data with the theory described in the previous paper (1), we have to assign physically realistic values to the various parameters. The most important ones are the dimensions of the lattice cell and the non-electrostatic polymer-solvent interaction parameter. It is found that a reasonable choice for these parameters can be made, such that the theoretical model predicts the measured increase of the adsorbed amount with c_s and log r. The quantitative difference between theory and experiment amounts to only 35 %. This is acceptable, considering the large number of parameters involved and the uncertainty in their estimates. Moreover, it is not certain that the same specific surface area applies for PSS and for the nonionic surfactant used before (8).

Choice of parameters

The lattice theory for polyelectrolyte adsorption is characterized by nine parameters (1). Two of these, the fraction λ_0 of nearest neighbours of a site in the same layer and the edge r_o of the lattice cell, characterize the lattice. Four additional parameters are required for the description of the polyelectrolyte solution: the polyelectrolyte concentration ϕ_*, the salt concentration c_s, the number r of segments per chain and the non-electrostatic segment-solvent interaction χ. The presence of an adsorbing surface is accounted for by the remaining three parameters, the surface charge density σ_o, the thickness r_s of the charge-free Stern layer adjacent to the surface and the adsorption energy χ_s.

The geometry of the lattice is completely determined by the parameter λ_0. For a lattice with coordination number z, each site has z nearest neighbours, of which $\lambda_0 z$ are situated in the same lattice layer and $\lambda_1 z$ in each of the two adjacent layers ($\lambda_0 + 2\lambda_1 = 1$). Variations in the lattice geometry are only of minor importance in the theory (6). Therefore, we consider only a hexagonal lattice, for which $\lambda_0 = 0.5$ (and $z = 12$).

When the dimension r_o of the lattice cell is known, theoretical adsorption data (θ_{ex}, in equivalent monolayers or segments per surface site) may be compared to experimental results (Γ, in monomole/g), provided the specific surface area of the adsorbent is known. For uncharged polymers θ_{ex} itself does not depend on r_o. However, for polyelectrolytes the electrostatic interactions depend on r_o and, therefore, the value ascribed to r_o is far more important. The segmental charges are thought to be smeared out in parallel planes situated at the center of the lattice cells, and the separation r_o between these planes affects the potential in the system and thus also θ_{ex}. In order to estimate r_o, we first consider the unperturbed persistence length of the PSS chain. This parameter represents the intrinsic stiffness of the chain and is a measure for the length of a chain part that is completely flexible. This length is related to r_o since the model chain is also assumed to be completely flexible. Stigter (12) gives a value of 1 nm for the persistence length of an unperturbed PSS chain. A distance of 1 nm along the backbone corresponds to four monomeric units, as the effective length of two C-C bonds is around 0.25 nm. Due to the large side groups a sequence of four monomeric units constitutes a roughly isotropic lattice cell. Hence, we assume that one theoretical segment corresponds to four monomeric units. From the specific volume of PSS (13), a monomer volume of 0.2 nm^3 is calculated, giving a volume of 0.8 nm^3 for a theoretical segment. The edge of a cubic of 0.8 nm^3 is 0.93 nm, which we adopt as the value for r_o. The latter value agrees well with the persistence length given by Stigter, and we conclude that our estimation is internally consistent.

One would expect that a lattice cell containing four monomeric units also comprises four elementary charges, since PSS is a strong polyelectrolyte. Manning (14) showed, however, that the charge density

along a linear polyelectrolyte cannot exceed a critical value. This limiting charge density corresponds to a minimum separation between successive charges that is equal to the Bjerrum length b. For a chain on which the spacing between the charges is smaller than b, it is envisaged that counterion condensation occurs until the effective charge distance equals b. If the relative dielectric permittivity ε_r around a segment is taken as that of water, b = 0.71 nm. In a polyelectrolyte chain, though, a monomeric unit is not entirely surrounded by water. At least two of its nearest neighbours are chain segments, and the relevant value for ε_r is some average of the value for water (ε_r = 80) and that of the styrene sulfonate unit (15). For the latter, ε_r = 8 seems to be a reasonable estimate (16). In a hexagonal lattice, there are twelve nearest neighbours of which at most ten contain solvent, so we find as the maximum value for the average relative dielectric permitivity: ε_r = (2*8 + 10*80)/12 = 68. The minimum Bjerrum length is, therefore, b = (80/68)*0.71 = 0.84 nm, which differs not too much from r_0. We conclude that three of the four monomeric units in a lattice cell can be considered to be effectively uncharged due to counterion condensation. Since there is left one elementary charge per segment, we have effectively α = 1, also for the model chain.

In a polyelectrolyte solution the first parameter to consider is the concentration of the polyelectrolyte. Experimentally it is used in units monomole/l, whereas in the model it is expressed as the dimensionless volume fraction. The conversion factor between experimental and theoretical units is the specific volume of the monomeric unit. For NaPSS, Boyd (12) gives a value of 112 ml/monomole.

As the indifferent electrolyte we used NaCl. Contrary to the polyelectrolyte segments, the small ions are treated as point charges in the model; their concentration is expressed in mole/l.

The number of lattice cells r occupied by a PSS chain is $M/4M_{mon}$, where M is the molecular weight as specified by the manufacturer, excluding the sodium counterion, and M_{mon} (= 0.196 kg/mole) the molecular weight of the monomeric unit, also without the counterion.

The interaction of a polyelectrolyte segment with the solvent (a solution of indifferent electrolyte in water) includes an electrostatic and a non-electrostatic component that are, to a first approximation, mutually independent. The first is accounted for by smearing out the

segmental charges in parallel planes and solving the resulting Poisson-Boltzmann equation for the potential (1), whereas the latter is characterized by the Flory-Huggins χ-parameter (17). The two contributions to the segment-solvent interaction cannot be distinguished experimentally. In order to find χ, measurements have to be carried out that can be interpreted using a model in which non-electrostatic and electrostatic segment-solvent interactions are treated separately. Such a model is given by Van der Schee for the description of phase separation in polyelectrolyte solutions (4). Experimental data on the phase separation behaviour of PSS are available from Takahashi et al. (18).

Van der Schee's analysis of phase separation in polyelectrolyte solutions is based on Flory's model for uncharged polymers (17). A solution containing uncharged polymer may separate into two coexisting phases of different composition, when χ is above a critical value χ_{cr}:

$$\chi_{cr} = (1 + 1/\sqrt{r})^2/2 \qquad [1]$$

For long chains, $\chi_{cr} \cong 0.5$. Flory's lattice model for the polymer solution was extended by Van der Schee (4) to include polyelectrolytes. This can be achieved in a very simple way when the Debye-Hückel (DH) approximation may be applied (potentials lower than 50 mV throughout the system). It was shown that the Flory expression for the free energy of mixing remains valid for polyelectrolytes, provided that χ is replaced by an effective χ-parameter χ_{eff} which incorporates the non-electrostatic interaction parameter (χ) and an electrostatic term (ξ):

$$\chi_{eff} = \chi - \xi \qquad [2]$$

Again the conditions under which phase separation occurs can be predicted using eq. [1]: $\chi_{eff} > \chi_{cr} \cong 0.5$ for long polyelectrolyte chains.

With polyelectrolytes in water χ may be large because a polyelectrolyte segment, apart from the charged group, is usually hydrophobic. The electrostatic segment-solvent interaction improves the solubility of the polyelectrolyte, so that ξ is positive and $\chi_{eff} < \chi$.

Smearing out the segmental charges in planes parallel to the surface, through the center of the lattice cell yields:

$$\xi = \frac{\alpha^2 e^2}{4\varepsilon\kappa r_o^2 kT} \frac{1 + \exp(-\kappa r_o)}{1 - \exp(-\kappa r_o)} \qquad [3]$$

where e is the proton charge and κ the reciprocal thickness of the electrical double layer:

$$\kappa^2 = (\bar{n}_+^+ + \bar{n}_-^+)e^2/\varepsilon kT \qquad [4]$$

expressed in terms of stoichiometric concentrations of small ions in the reference phase ($\bar{n}_+^+$, $\bar{n}_-^+$). This reference phase may be either one of the two coexisting phases, each of which has its own concentrations of polyelectrolyte and small ions. Consequently in eq. [4] we face one of the major imperfections inherent to the DH-approximation: the equations are not invariant with the choice of the reference phase. Only at very low c_s, where the concentrations of indifferent electrolyte and polyelectrolyte are comparable, will this have practical implications. Eq. [3] was made available to us by Van der Schee in a personal communication. In his thesis (4), a different expression for ξ is given applying to completely homogeneous polyelectrolyte solutions (the classical Donnan model). Here it seems more appropriate, though, to use a model for the solution in which the charges are concentrated on parallel plates, since that approach is also used for the polyelectrolyte adsorption theory. The derivation of Eq. [3] will be published separately.

As stated above, incipient phase separation occurs if $\chi_{eff} \cong 0.5$ or:

$$\chi \cong 0.5 + \xi \qquad [5]$$

For very long PSS molecules, in NaCl solution at 25 °C, Takahashi et al. (18) reported the onset of phase separation at 4.2 M NaCl. Assuming $\alpha = 1$ and $r_o = 0.93$ nm we obtained from eq. [3] $\xi = 0.33$, so that χ is found as 0.83. This value is, strictly speaking, only valid at 4.2 M NaCl, whereas our adsorption experiments were carried out at lower ionic strength (0.5 M $\leq c_s \leq$ 3.5 M). Properties of the solvent obviously

change with c_s and it could be envisaged that, apart from ξ, also the non-electrostatic component χ varies with the ionic strength. However, we do not have any independent information on this dependence, and therefore we will assume a constant value, $\chi = 0.8$, which is slightly below that at the onset of phase separation. At any rate, it is clear that even at high c_s electrostatic interactions cannot be neglected in polyelectrolyte solutions, ξ being around 0.3 in 4 M NaCl.

In the presence of an adsorbing surface, also the remaining three parameters (σ_0, r_s and χ_s) are needed to describe the system completely. POM crystals, of which the surface consists entirely of ether groups ($-CH_2O-$), are essentially uncharged (8) and therefore we take $\sigma_0 = 0$. The thickness of the Stern layer may be estimated from the hydrated radius of the Na^+ ion, given by Robinson and Stokes (19) as 0.33 nm. Upon adsorption partial dehydration occurs and for r_s a value lower than 0.33 nm is expected. We assume $r_s = 0.25$ nm. Finally, the non-electrostatic adsorption energy parameter χ_s cannot be estimated a priori. Recently, Cohen Stuart et al. (20) proposed a method to assess χ_s by displacing adsorbed polymer from the surface by low molecular weight competing substances. However, the procedure is laborious and, so far, has only been applied for uncharged polymers. We regard χ_s as an adjustable parameter, choosing that value that gives a reasonable fit between theory and experiment. The adopted value is 0.65, corresponding to a low adsorption energy. This is not surprising for an organic surface with weak dispersion forces. For the high-energy surface of AgI, Van der Schee and Lyklema (5) use $\chi_s = 4.86$.

Experimental adsorption data (Γ) are obtained in monomole/g, whereas theoretical calculations yield the adsorbed amount (θ_{ex}) in equivalent monolayers or segments per surface site. The trends in Γ may be compared directly to those in θ_{ex}. However, in order to relate the experimental adsorption quantitatively to theoretical data, we need the adsorbed amount, in monomole/g, that corresponds to a complete monolayer of lattice cells (Γ_{mon}). One segment per lattice site corresponds to four monomeric units per 0.93^2 nm^2 or $7.68 * 10^{-6}$ monomole/m^2. Since the specific surface area of the POM crystals is 60 m^2/g, $\Gamma_{mon} = 4.61 * 10^{-4}$ monomole/g, which can be used as the conversion factor between θ_{ex} and Γ.

Results and discussion

In figs. 1-3 we compare experimental adsorption data (dashed curves), obtained for NaPSS on POM single crystals in the presence of NaCl, with the predictions of the lattice model (full curves). We use two different ordinate scales, the left one for the experimental adsorption Γ, in monomole/g and the right one to represent the theoretical results θ_{ex}, expressed in equivalent monolayers. In this way we avoid the explicit use of the conversion factor Γ_{mon}, which might well be wrong by 50 %, and yet theoretical and experimental trends can be compared directly.

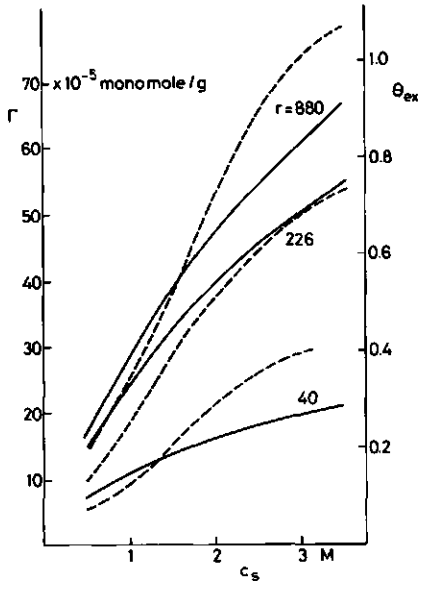

Figure 1: Adsorption as a function of ionic strength at $\phi_* = 67$ ppm. Full curves indicate theoretical results (θ_{ex}, in equivalent monolayers) and dashed curves represent experimental data (Γ, in monomole/g). The values assigned to model parameters are given in the text.

The dependence of the adsorption on the salt concentration c_s is given in fig. 1. At constant polyelectrolyte concentration, c_s is varied between 0.5 M and 3.5 M for three molecular weights. The conversion factor between the number of segments r per chain and the molecular weight M was taken as $4M_{mon}$ ($r = M/4M_{mon}$), as discussed above. We see a roughly linear increase of the adsorption with c_s, both experimentally and theoretically. The experimental result was described before (11) as typical for adsorption on a low-energy, uncharged

surface. Under these conditions a high ionic strength is required for any adsorption to occur at all.

The theoretical curves in fig. 1 reproduce the increase of the measured adsorption with c_s satisfactorily. This supports the way in which the electrostatic interactions are incorporated in the theoretical model. However, it is observed that the experimental ionic strength dependence is somewhat stronger than the theoretical one. As a consequence we found good agreement either at low c_s (r = 40, 880) or at high c_s (r = 226). A possible reason for this discrepancy is a solvent quality that varies with the salt concentration: the non-electrostatic interaction between segments and water is probably different from that between segments and hydrated salt ions. If we would assume an increase of χ with increasing c_s, the theoretical curves would become steeper and the agreement with experiment would improve. Similarly, χ_s could be a function of salt concentration. Since we have no independent evidence for the dependence of χ or χ_s on ionic strength, we will not pursue this point any further.

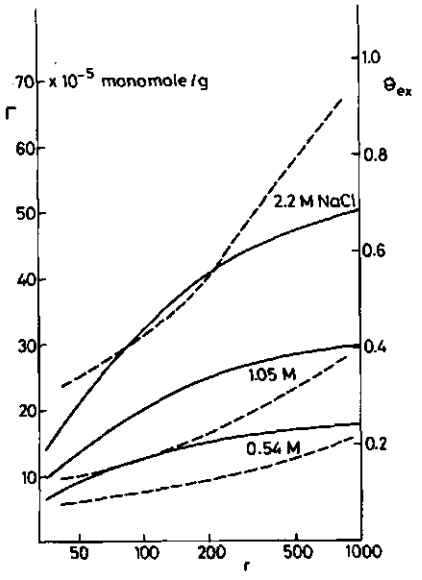

Figure 2: Adsorption as a function of chain length at $\phi_* = 67$ ppm. As in fig. 1, full curves are theoretical results and dashed curves are experimental.

In fig. 2 we give the adsorbed amount as a function of the chain length at three salt concentrations. Experimentally, a distinct increase of the adsorption with r is obtained and the theoretical

calculations confirm this trend. The increase is related to the low affinity of the segments for the POM surface (11). The increase of the experimental adsorption with the chain length is stronger than that predicted by theory. Especially at the highest ionic strength, where the adsorbed amount is also highest, the theoretical curve levels off too strongly for large r. This feature is probably a consequence of the use of the Roe model for uncharged polymer (6) as the basis of the present theory. In his analysis Roe neglects the occurrence of free dangling tails at either end of an adsorbed polymer molecule. Scheutjens and Fleer (21) demonstrated that for long chains this simplification results in serious underestimation of the adsorbed amount. With polyelectrolyte adsorption this effect will be most pronounced at high c_s, where the electrostatic repulsion between segments becomes small and the structure of the adsorption layer is very similar to that of uncharged polymer (1). A major improvement in the theory would be the replacement of Roe's model by that of Scheutjens and Fleer (21), in which tails are explicitly accounted for. Although this can be done in principle (4,5), so far the numerical complications of the extended Scheutjens-Fleer model have not been solved completely.

For the lower salt concentrations the theoretical curves are higher than the experimental ones. In the discussion of the dependence of the adsorption on c_s, we mentioned already that a better agreement would be obtained if χ and/or χ_s are considered a function of c_s.

In fig. 3 the dependence of the adsorbed amount on the polyelectrolyte concentration is presented, for three salt concentrations and r = 226. The measured isotherms are rounded, whereas theoretically high-affinity isotherms are obtained. We described the experimental isotherms before (11), and explained their low-affinity character as a consequence of weak interaction with the low-energy, uncharged POM surface. Theoretically, always flat isotherms are found, irrespective of the surface-polyelectrolyte interaction and the ionic strength (1). The poor agreement between theory and experiment in fig. 3, and in particular the fact that roundedness is not found in the theoretical isotherms, may be a consequence of the application of the lattice model for the bulk solution. This is only justified in case of significant interpenetration of the individual polyelectrolyte molecules, which is not likely to occur at the volume fractions where

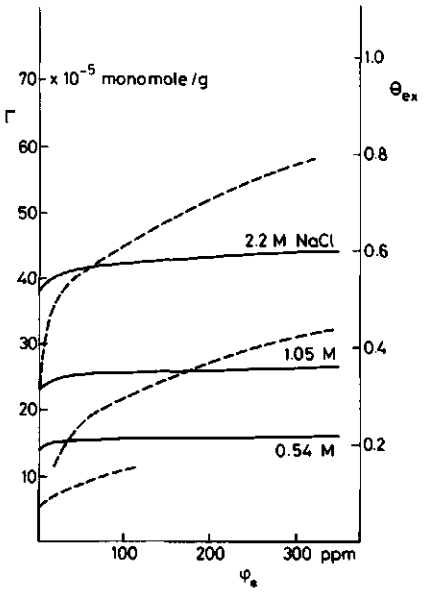

Figure 3: Adsorption as a function of polyelectrolyte concentration for r = 226. Full curves are theoretical, dashed curves experimental.

adsorption experiments are carried out ($\phi_* < 500$ ppm). Therefore, the poor agreement obtained as to the shape of the isotherms is perhaps a fallacy of the theory, due to the description of the bulk solution with a lattice model, even at low ϕ_*. In this way a wrong concentration dependence could be introduced. However, at present it seems difficult to improve the theory in this respect.

So far, we have only compared the general trends of the adsorbed amount as a function of ionic strength, chain length and solution concentration. A more quantitative comparison is possible by relating the left hand side and right hand side ordinate scales of figs. 1 - 3 by means of the conversion factor Γ_{mon}. In this way it is found that theoretical and experimental adsorption data differ by about 35 %. This result is encouraging in view of the large number of model parameters and the approximations involved in their assessment. Also, the specific surface area of the POM suspension might be subject to considerable error. This is illustrated by the fact that we found previously a geometric surface area of 150 m^2/g, whereas BET analysis of nitrogen gas adsorption data yielded 30 m^2/g (8). In suspension the surface area was obtained from the adsorption plateau of a non-ionic surfactant, giving

60 m^2/g.

Our results are in line with those of Marra et al. (7) for PSS on preheated silica. In both cases the model qualitatively confirms the measured dependence of adsorption upon ionic strength and molecular weight. Rounded isotherms cannot be reproduced with the model, neither with the set of parameters applied by Marra et al., nor with the values reported in this paper.

Conclusions

Experimental adsorption data obtained for PSS on POM single crystals in concentrated NaCl solutions are compared with a new lattice theory for polyelectrolyte adsorption. The model involves nine parameters. The most important of these are the size of a lattice cell r_o, which affects the electrostatic interactions, the non-electrostatic polymer-solvent interaction parameter χ and the segmental adsorption energy parameter χ_s. The edge r_o of the lattice cell was estimated by combining the persistence length of the PSS chain with the specific volume of a monomeric unit. We concluded that each cell contains four monomeric units. Effectively, only one of these four monomers carries a charge, due to the occurrence of counterion condensation. Therefore the degree of dissociation of the model chain is still unity. The value of χ was estimated from a theoretical interpretation of phase separation data, giving $\chi \cong 0.8$. All errors in the parent model for the solution and in the way electrostatic interactions are incorporated, will accumulate in this value for χ. We therefore use it merely as a first estimate. Finally, χ_s was treated as an adjustable parameter.

The measured increase of the adsorbed amount as a function of ionic strength and molecular weight is qualitatively reproduced by the theory. This shows that the combination of electrostatic interactions and conformational statistics is, in principle, correctly accounted for in the model. Yet, the experimental dependence is in both cases somewhat stronger than predicted theoretically. With respect to the ionic strength dependence, this might be a consequence of variations in χ or χ_s upon changing the salt concentration. In the simple model applied in this paper, χ_s and χ were considered constant.

Theoretical θ_{ex} - r curves level off for high r, probably because the occurrence of tails at either end of an adsorbed polyelectrolyte chain is neglected in the model. At high c_s this effect is most pronounced. Under these conditions segment-segment repulsion is small and the adsorbed chains behave more or less like uncharged polymer, with a large part of the segments in loops and tails. Neglect of tails is inherent to Roe's theory for adsorption of uncharged polymer, used as the parent model in this analysis of polyelectrolyte adsorption. Replacement by the theory of Scheutjens and Fleer, in which tails are explicitly accounted for, would probably improve the theoretical results in this respect.

Experimental adsorption isotherms for PSS on POM crystals are rounded, whereas theoretically high-affinity character is expected. The discrepancy may be due to the assumption of a lattice model for the bulk solution, despite the very low concentration of polyelectrolyte used in adsorption experiments (< 500 ppm).

For a quantitative test of the theory we used Γ_{mon}, the adsorbed amount in a complete monolayer expressed in monomole/g, as the conversion factor between theoretical units (equivalent monolayers) and experimental units (monomole/g). The difference between theory and experiment turned out to be of the order of 35 %, which is satisfactory in view of the uncertainties in the various parameters and in the specific surface area of the adsorbent.

Acknowledgement

We thank Dr. H.A. van der Schee for his advice concerning the application of his polyelectrolyte adsorption theory.

References

1. Papenhuijzen, J., Van der Schee, H.A., and Fleer, G.J., J. Colloid Interface Sci., part I of this paper.
2. Hesselink, F.Th., J. Electroanal. Chem. 37, 317 (1972).
3. Hesselink, F.Th., J. Colloid Interface Sci. 60, 448 (1977).

4. Van der Schee, H.A., Thesis Agricultural University, Wageningen, 1984.
5. Van der Schee, H.A., and Lyklema, J., J. Phys. Chem., submitted.
6. Roe, R.-J., J. Chem. Phys. 60, 4192 (1974).
7. Marra, J., Van der Schee, H.A., Fleer, G.J., and Lyklema, J., in "Adsorption from Solution," (R.H. Ottewill, C.H. Rochester and A.L. Smith, Eds.), p. 245. Academic Press, London, 1983.
8. Papenhuijzen, J., and Fleer, G.J., J. Colloid Interface Sci., in press.
9. Cohen Stuart, M.A., Scheutjens, J.M.H.M., and Fleer, G.,J., J. Polym. Sci. Polym. Phys. Ed. 18, 559 (1980).
10. Papenhuijzen, J., Thesis Agricultural University, Wageningen, in preparation.
11. Papenhuijzen, J., Fleer, G.J., and Bijsterbosch, B.H., J. Colloid Interface Sci., submitted.
12. Stigter, D., Macromolecules 15, 635 (1982).
13. Boyd, G.E., J. Chem. Eng. Data 22, 413 (1977).
14. Manning, G.S., J. Chem. Phys. 51, 924 (1969).
15. Böttcher, C.J.F., "Theory of Electric Polarization," Elseviers Publishing Company, Inc., Amsterdam, 1952.
16. Handbook of Chemistry and Physics 56th ed., R.C. Weast, Ed., table E56-58, CRC Press, Inc., Cleveland, 1975.
17. Flory, P.J., "Principles of Polymer Chemistry," p. 508 and 544. Cornell University Press, Ithaca, 1953.
18. Takahashi, A., Kato, T., and Nagasawa, M., J. Phys. Chem. 71, 2001 (1967).
19. Robinson, R.A., and Stokes, R.H., "Electrolyte Solutions," p. 121. Butterworths, London, 1955.
20. Cohen Stuart, M.A., Fleer, G.J., and Scheutjens, J.M.H.M., J. Colloid Interface Sci. 97, 515 and 526 (1984).
21. Scheutjens, J.M.H.M., and Fleer, G.J., J. Phys. Chem. 83, 1619 (1979) and 84, 178 (1980).

SUMMARY

The objective of the present work was to collect systematic adsorption data for a well-defined polyelectrolyte on an uncharged, homogeneous surface, and to compare these with the new theory that was recently developed by Van der Schee.

In chapter 1 we shortly describe which factors determine the adsorption equilibrium. Understanding these in relation to their interplay is, ultimately, of great importance in numerous practical applications of adsorbing polyelectrolytes. Subsequently, we introduce the model system: polyoxymethylene (POM) single crystals as the adsorbent and polystyrene sulfonate (PSS) as the adsorbate.

The preparation and characterization of the adsorbent is discussed in chapter 2. Single crystals of POM are flat, homogeneous and essentially uncharged, and offer a large specific surface area. Since they can be prepared reproducibly and in large amounts, they constitute a suitable model substrate in systematic adsorption studies. The crystallization procedure is discussed in some detail. The thickness of the crystals is obtained from EM and SAXS measurements, the results being in excellent mutual agreement. Combining this thickness with the crystal density the geometrical surface area is found to be 150 m^2/g. This is compared with the surface area obtained by BET analysis of nitrogen adsorption (30 m^2/g) and with the surface area that follows from adsorption of polyoxyethylated nonyl phenols from aqeous solution (60 m^2/g). The discrepancy in the results is explained in terms of different degrees of aggregation of POM crystals in the dry state and in suspension. Finally, some preliminary results of albumin and PSS adsorption are discussed.

We characterized ten commercial samples of homodisperse PSS by elemental analysis, measurement of the extinction coefficient and viscometry. From the results, presented in chapter 3, we conclude that only five of them are sufficiently reliable. For these the degree of sulphonation is 97.5 %, the extinction coefficient at λ = 226 nm amounts to 11,600 $M^{-1}cm^{-1}$, and the intrinsic viscosities in 0.5 M NaCl conform

to the Mark-Houwink relation with K = 1.087 g/g and a = 0.764.

Systematic measurements of adsorption as a function of polyelectrolyte concentration, chain length and ionic strength are reported in chapter 4. Substantial adsorption occurs only at high ionic strength, as a consequence of the low affinity of the PSS for the POM surface. Adsorption isotherms are rounded. The adsorption increases more or less linearly with increasing ionic strength, and also we find a relatively strong dependence upon the molecular weight. From a comparison with adsorption results on hematite and with literature data on other systems, clear trends emerge as to the relation between adsorption characteristics and the affinity of the polyelectrolyte for the surface. This affinity may have both electrostatic and non-electrostatic components. With increasing affinity, isotherms become flatter, the molecular weight dependence weaker, and the effect of ionic strength smaller. Desorption experiments showed that the adsorption of PSS on POM is essentially reversible.

Chapter 5 deals with polyelectrolyte adsorption theories. These may be derived from models for adsorption of uncharged polymers by incorporating the electrostatic free energy in the partition function of the system. We show in some detail how the lattice model of Roe for adsorption of uncharged polymers is extended to polyelectrolyte adsorption by Van der Schee. Systematic calculations based upon the new theory were performed. Major features are the high affinity character of adsorption isotherms, under all conditions, and the profound influence of the ionic strength upon the adsorption behaviour. At high salt concentration, the adsorption increases more strongly with ionic strength and molecular weight than at low salt concentration, and also the non-electrostatic segment-solvent interactions, expressed in the χ-parameter, are more important. The non-electrostatic surface-polyelectrolyte affinity parameter χ_S has a marked effect for any ionic strength. When either χ_S or the salt concentration is low, the adsorption remains well below monolayer coverage. In that situation the presence of a surface charge of opposite sign to that of the polyelectrolyte gives rise to an additional adsorption of one (univalent) segment per elementary charge on the surface (charge compensation). For the thickness of the adsorbed layer we find 2 - 5 nm.

Finally, in chapter 6 we compare experimental adsorption data for PSS on POM crystals with a recent lattice theory for polyelectrolyte adsorption. The dimensions of a lattice cell are estimated from the specific volume of the PSS monomer in combination with the persistence length of the chain, and the non-electrostatic segment-solvent interaction parameter χ is assessed from literature data on phase separation. Qualitatively, the model reproduces the measured increase of adsorption with ionic strength and molecular weight. However, experimentally the adsorption increases more strongly than theoretically. For the ionic strength dependence we ascribe this to some variation of the solvent quality (χ) or the segment-surface interaction (χ_s) with the salt concentration. The theoretical increase of adsorption with molecular weight is probably too weak because the occurrence of free dangling tails at either end of an adsorbed chain is neglected in the Roe model. Experimental isotherms are rounded, whereas theoretically high-affinity isotherms are found. This may be a consequence of applying a lattice model for the bulk solution. The quantitative difference between experimental and theoretical adsorption is around 35 %, a satisfactory result in regard of the large number of model parameters and the uncertainties in their estimated values. Moreover, also the specific surface area of the adsorbent is liable to considerable error.

SAMENVATTING

In dit proefschrift worden systematische adsorptiemetingen beschreven, uitgevoerd met een goed gedefinieerd polyelectrolyt en een adsorbens waarvan het oppervlak homogeen is en ongeladen. De belangrijkste doelstelling van het werk bestaat in de vergelijking van experimentele resultaten met een nieuwe theorie, die onlangs door Van der Schee is ontwikkeld.

In hoofdstuk 1 beschrijven we kort de factoren die het adsorptie gedrag van polyelectrolyten bepalen. Een goed begrip hiervan en van hun onderlinge samenhang is uiteindelijk van groot belang in vele praktische toepassingen van adsorberende polyelectrolyten. Vervolgens introduceren we het gebruikte modelsysteem: polyoxymethyleen (POM) eenkristallen als adsorbens en polystyreensulfonaat (PSS) als adsorbaat.

Bereidingswijze en karakteristieken van het adsorbens komen aan de orde in hoofdstuk 2. Het oppervlak van POM-eenkristallen is vlak, homogeen en praktisch ongeladen, en de kristallen bezitten een groot specifiek oppervlak. Als modelsysteem in systematische adsorptiemetingen zijn ze mede aantrekkelijk omdat bereiding in grote hoeveelheden op reproduceerbare wijze kan plaats vinden. Het kristallisatieproces wordt uitvoerig besproken. Meting van de kristaldikte door middel van EM en SAXS leverde vrijwel hetzelfde resultaat. In combinatie met het soortelijk gewicht van de kristallen volgt een waarde van 150 m^2/g voor het geometrisch oppervlak. We vergelijken dit met de uitkomst verkregen door BET-analyse van N_2-adsorptie (30 m^2/g) en met het oppervlak dat volgt op grond van adsorptiemetingen met polyoxyethyleennonylphenol in waterige oplossing (60 m^2/g). De sterk uiteenlopende resultaten vinden waarschijnlijk hun verklaring in een verschillende mate van aggregatie van droge POM kristallen in vergelijking met de toestand in suspensie. Dit hoofdstuk wordt besloten met een kort verslag van voorlopige adsorptiemetingen met albumine en PSS.

We karakteriseerden tien commercieel verkrijgbare, homodisperse PSS-monsters door middel van elementen-analyse, bepaling van de extinctiecoefficient en viscosimetrie. Op grond van de bevindingen, zoals weergegeven in hoofdstuk 3, kan worden geconcludeerd dat slechts vijf monsters voldoende betrouwbaar zijn. De sulfoneringsgraad hiervan bedraagt 97,5 % en de extinctiecoefficient 11.600 $M^{-1}cm^{-1}$ (λ = 226 nm). De intrinsieke viscositeiten in 0,5 M NaCl voldoen aan de Mark-Houwink relatie met K = 1,087 g/g (molecuulgewicht in kg/mol) en a = 0,764.

Systematische adsorptiemetingen als functie van de polyelectrolytconcentratie, ketenlengte en ionsterkte worden behandeld in hoofdstuk 4. Alleen bij hoge ionsterkte is adsorptie meetbaar. Dit is het gevolg van de lage affiniteit van het PSS voor het POM-oppervlak. Adsorptie-isothermen hebben een ronde vorm. De adsorptie neemt min of meer lineair toe met oplopende zoutconcentratie, en ook vinden we een relatief sterke afhankelijkheid van het molecuulgewicht. Een vergelijking met adsorptiemetingen op hematiet en met resultaten uit de literatuur geeft een duidelijk beeld van het verband tussen trends in het adsorptiegedrag en de affiniteit van het polyelectrolyt voor het oppervlak. Deze affiniteit heeft zowel electrostatische als niet-electrostatische componenten. Met toenemende affiniteit worden de isothermen vlakker, vermindert de molecuulgewichtsafhankelijkheid en wordt de invloed van de ionsterkte kleiner. Desorptie-experimenten tonen aan dat adsorptie van PSS op POM kristallen reversibel is.

Hoofdstuk 5 handelt over theoretische modellen voor polyelectrolytadsorptie. Deze zijn zonder uitzondering gebaseerd op theorieen voor de adsorptie van ongeladen polymeren, door uitbreiding van de toestandssom van het systeem met een term voor de electrostatische vrije energie. Wij gaan in detail in op de adsorptietheorie die Van der Schee ontwikkeld heeft, uitgaande van het roostermodel van Roe voor ongeladen polymeren. We geven resultaten van systematische berekeningen met de nieuwe theorie. Belangrijke uitkomsten zijn het hoge-affiniteitskarakter van de adsorptie-isothermen, onder alle omstandigheden, en de uitgesproken invloed van de ionsterkte op het adsorptiegedrag. Bij hoge zoutconcentratie neemt de geadsorbeerde hoeveelheid sterker toe met de ionsterkte en de ketenlengte dan bij lage zoutconcentratie. Ook de niet-electrostatische wisselwerking tussen polyelectrolyt en

oplosmiddel, uitgedrukt in de χ-parameter, is dan belangrijker. De parameter χ_s, die de niet-electrostatische affiniteit tussen oppervlak en polyelectrolyt weergeeft, heeft grote invloed bij iedere ionsterkte. Voor lage χ_s of lage zoutconcentratie blijft de bedekking van het oppervlak met polyelectrolyt ver beneden de complete monolaag. In die situatie leidt de aanwezigheid van een oppervlaktelading met een ladingsteken dat tegengesteld is aan dat van het polyelectrolyt tot een extra adsorptie van een segment per elementairlading op het oppervlak (ladingscompensatie). Voor de dikte van de geadsorbeerde laag vinden we een waarde van 2 - 5 nm.

Tot slot vergelijken we in hoofdstuk 6 experimentele adsorptiegegevens voor PSS op POM kristallen met de recente roostertheorie voor polyelectrolytadsorptie. Hiertoe worden eerst de afmetingen van de roostercel geschat op grond van het specifiek volume van een PSS monomeer, in combinatie met de persistentielengte van de keten. Een benadering voor de parameter χ, de niet-electrostatische wisselwerking tussen polyelectrolyt en oplosmiddel, volgt uit literatuurgegevens over fasescheiding. Kwalitatief reproduceert het model de gemeten toename van de adsorptie met ionsterkte en molecuulgewicht. Experimenteel neemt de adsorptie echter sterker toe dan theoretisch. Wat betreft de afhankelijkheid van de ionsterkte schrijven we dit toe aan een mogelijke variatie van de oplosmiddelkwaliteit (χ) of de affiniteit tussen polyelectrolyt en oppervlak (χ_s) met de zoutconcentratie. De theoretische toename van de adsorptie als functie van de ketenlengte is waarschijnlijk te zwak omdat het voorkomen van vrije staarten aan de uiteinden van een geadsorbeerde keten wordt verwaarloosd in het model van Roe. Experimentele isothermen zijn rond van vorm, terwijl theoretisch isothermen worden gevonden die wijzen op een hoge affiniteit tussen polyelectrolyt en oppervlak. Mogelijk is dit een gevolg van het feit dat de bulkoplossing wordt beschreven met een roostermodel, ondanks de lage polyelectrolyt concentraties hierin. Kwantitatief bedraagt het verschil tussen experimentele en theoretische adsorptie ongeveer 35 %. Dit is een bevredigend resultaat, gezien het grote aantal modelparameters en de onzekerheid in de geschatte waarden hiervoor. Bovendien kan de onbetrouwbaarheid in het specifiek oppervlak in het algemeen zeker 30 % bedragen.

CURRICULUM VITAE

Jos Papenhuijzen werd op 30 mei 1956 te 's-Gravenhage geboren. Hij behaalde daar in 1974 het gymnasium-β diploma aan het Christelijk Gymnasium Sorghvliet. Aansluitend begon hij zijn studie aan de Landbouwhogeschool te Wageningen, in de Moleculaire wetenschappen. In maart 1981 slaagde hij (met lof) voor het ingenieursexamen, met als hoofdvakken Fysische chemie en Biochemie, en als bijvak Proceskunde.

Per 1 mei 1981 trad hij voor een periode van drie jaar in dienst van de Landbouwhogeschool bij de vakgroep Fysische en Kolloidchemie. In deze periode verrichtte hij onder begeleiding van Prof. Dr. G.J. Fleer en Prof. Dr. B.H. Bijsterbosch het onderzoek waaruit dit proefschrift is voortgekomen.

Sinds 16 juni 1984 is hij werkzaam op de Afdeling Analytical Measurements van Océ-Nederland B.V. te Venlo.